

MULTIWAVELENGTH AND MULTIMESSEGER SIGNALS OF DARK MATTER

NICOLAO FORNENGO

Department of Theoretical Physics, University of Torino
and Istituto Nazionale di Fisica Nucleare (INFN) – Torino
Italy

UNIVERSITA'
DEGLI STUDI
DI TORINO



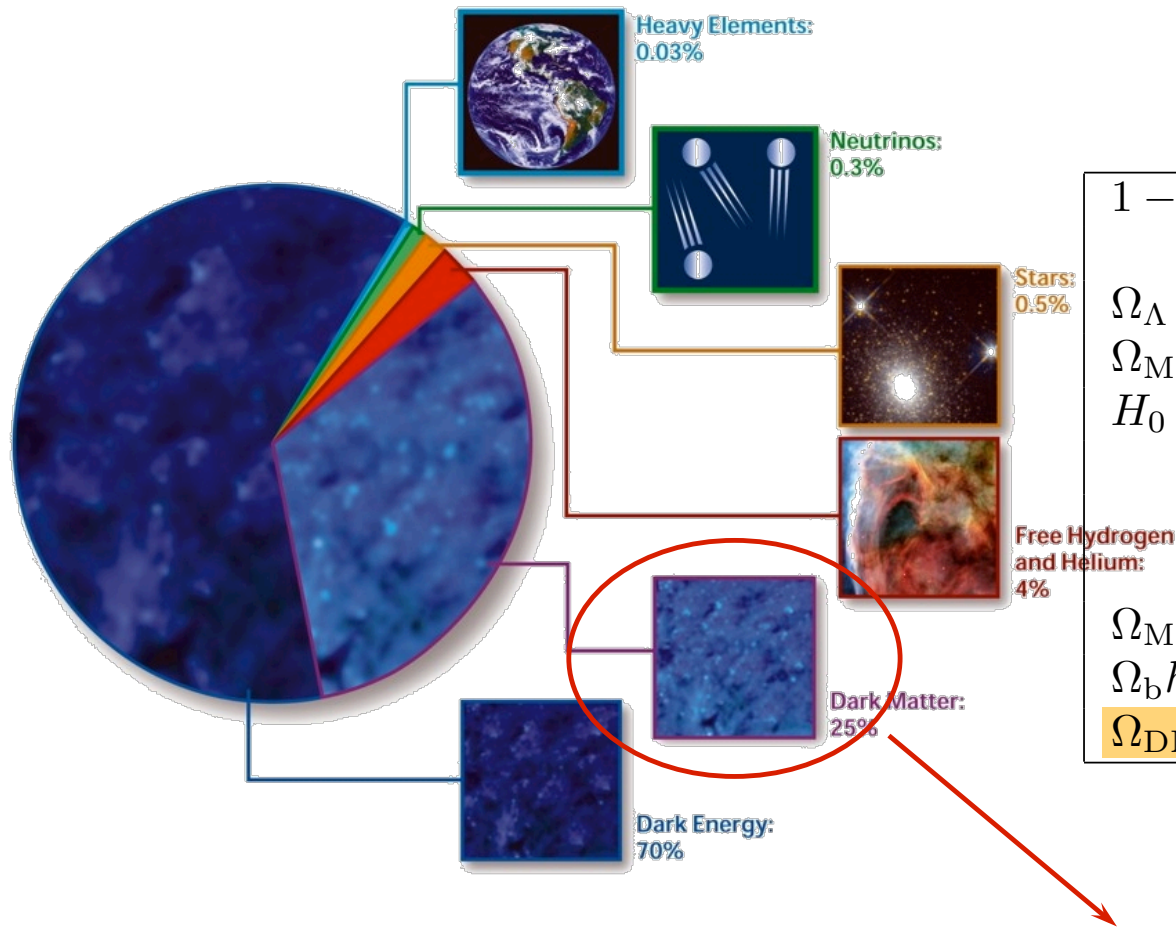
ALMA UNIVERSITAS
TAURINENSIS

fornengo@to.infn.it
nicolao.fornengo@unito.it

www.to.infn.it/~fornengo
www.astroparticle.to.infn.it



Dark Matter



$1 - \Omega_{\text{TOT}}$	-0.0105 ± 0.061	[95% C.L.]
Ω_{Λ}	0.693 ± 0.019	[68% C.L.]
Ω_{M}	0.307 ± 0.019	[68% C.L.]
H_0	67.9 ± 1.5	[95% C.L.]
	73.8 ± 2.4	[*]
	74.3 ± 2.6	[+]
$\Omega_{\text{M}} h^2$	0.1414 ± 0.0029	[68% C.L.]
$\Omega_{\text{b}} h^2$	0.02217 ± 0.00033	[68% C.L.]
$\Omega_{\text{DM}} h^2$	0.1186 ± 0.0031	[68% C.L.]

Ade et al. (Planck Collab.), arXiv: 1303.5076
 [*] Riess et al., Ap. J. 730 (2011) 119
 [+] Freedmann et al., Ap. J. 758 (2012) 24

Overwhelming evidence:

- Dynamics of galaxy clusters
- Rotational curves of galaxies
- Weak lensing
- Structure formation from primordial density fluctuations
- Energy density budget

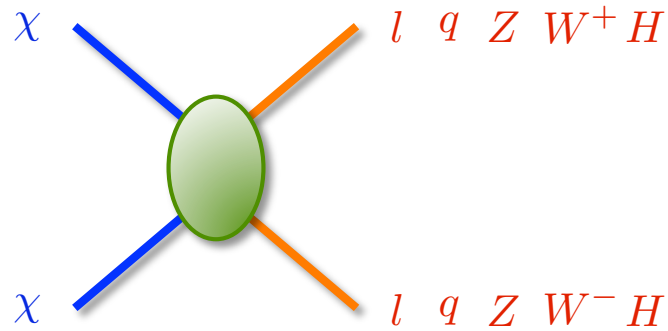
Non-baryonic (cold) dark matter is needed

- No candidate in the Standard Model
- New fundamental Physics

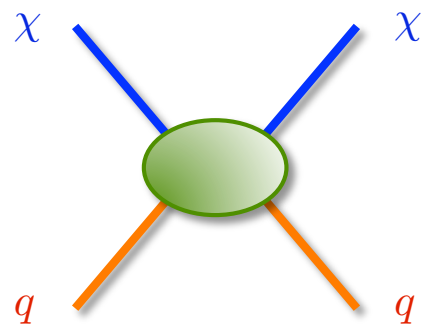
Two fundamental questions

- Identify the particle candidate
- Identify a non-gravitational signal

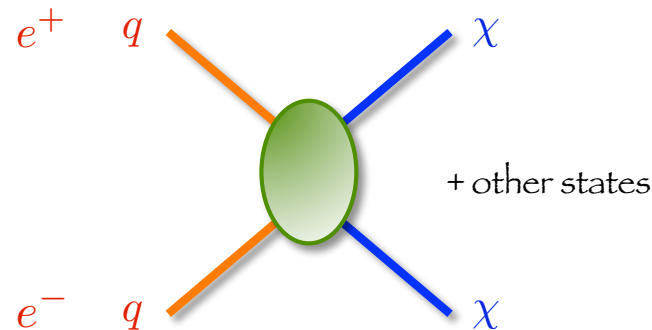
Mechanisms of DM signal production



Annihilation (or decay)

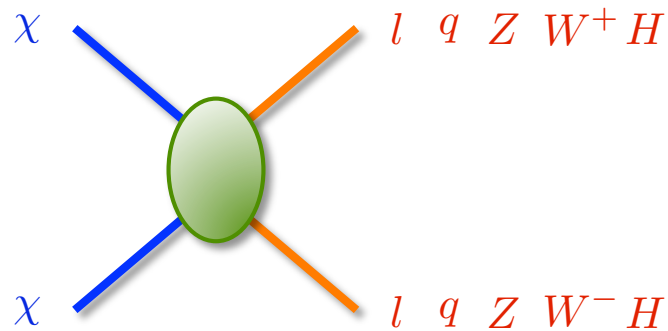


Scattering with ordinary matter



Accelerator searches

Indirect astrophysical signals

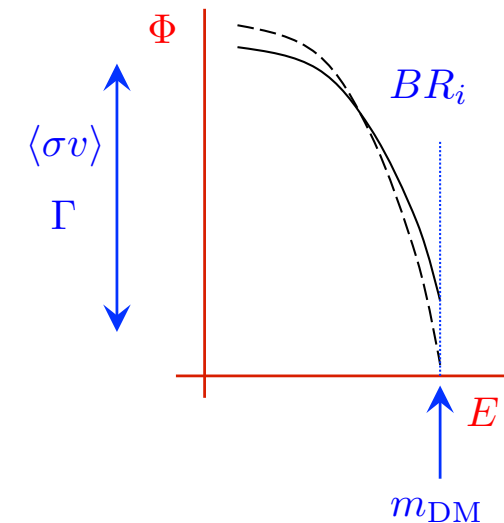


Annihilation (or decay)

Relevant particle physics properties:

1. Annihilation cross section (*) (or decay rate)
2. Mass of the DM particle
3. BR in the different final states

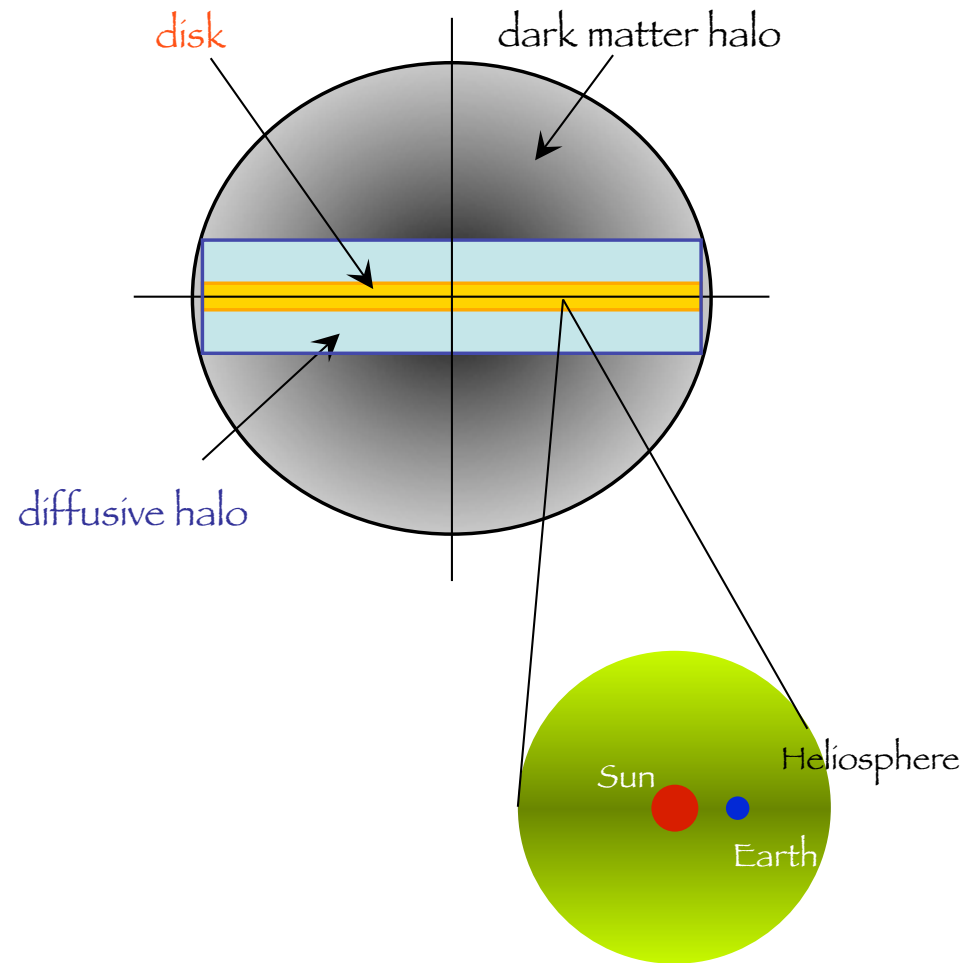
1 + 2 : Size of the signal
2 + 3 : Spectral features



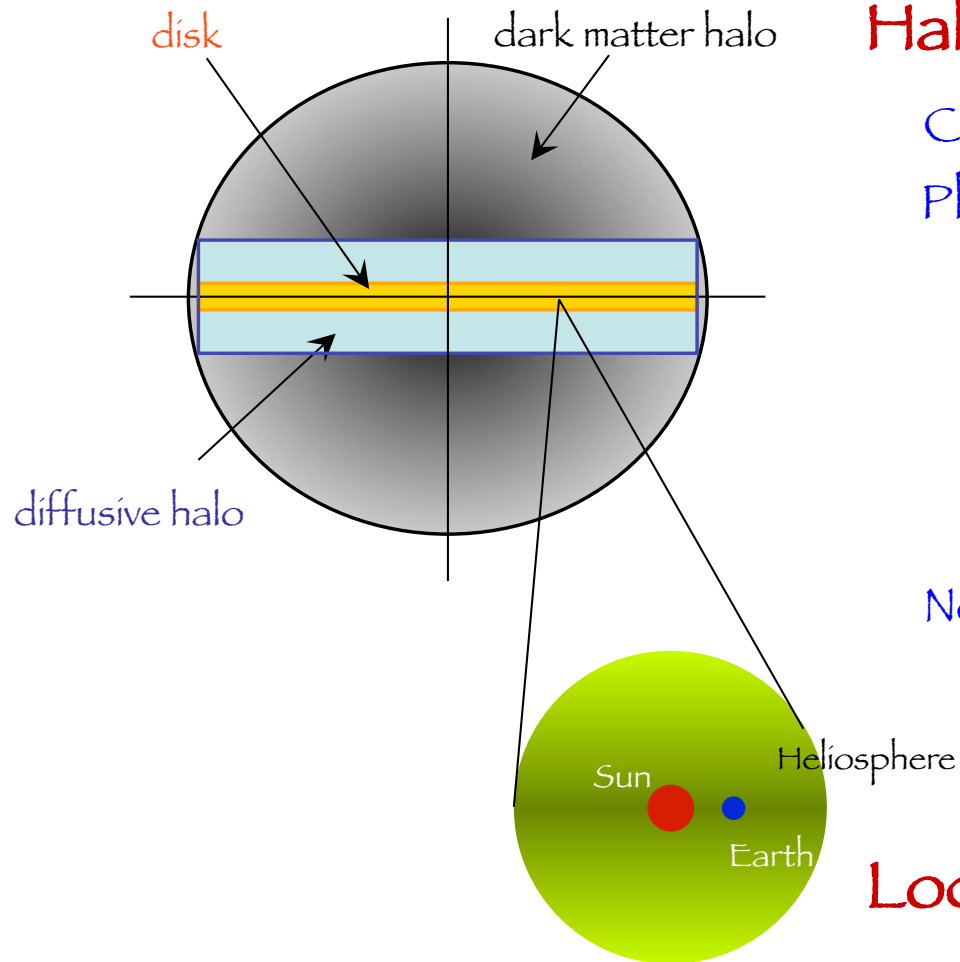
(*) Determines also the cosmological relic abundance (for a thermal DM)

$$\Omega h^2 = 0.11 \longleftrightarrow \langle\sigma_{\text{ann}}v\rangle = 2.3 \times 10^{-26} \text{ cm}^3 \text{ s}^{-1}$$

Galactic environment



Particle dark matter signals



Halo signals

Charged CR (e^+ , $anti p$, $anti D$)

Photons

- Gamma

- Prompt production

- IC from e^+/e^- on ISRF

- Radio

- Synchro from e^+/e^- on mag. field

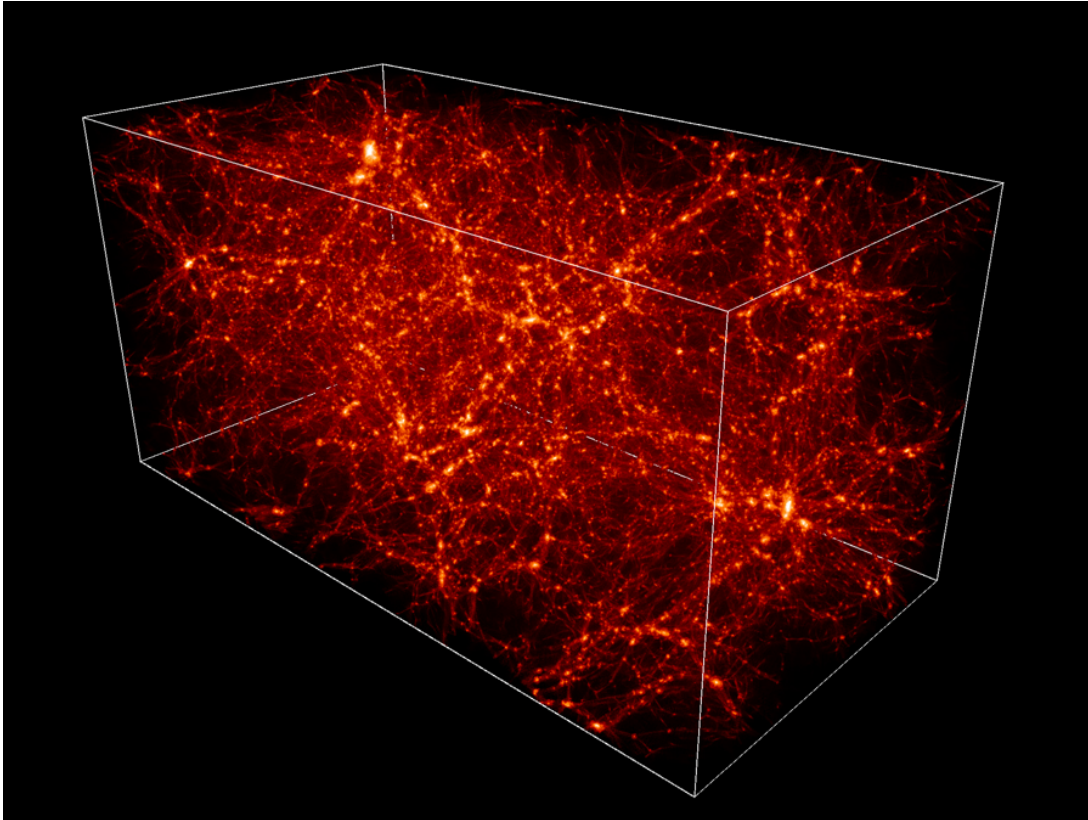
Neutrinos

Local signals

Direct detection

Neutrinos from Earth and Sun

Extra-galactic environment



Extragalactic signals

Photons: gamma, X, radio

Neutrinos

Sunyaev-Zeldovich effect on CMB

Optical depth of the Universe

Astrophysical dark matter signals

Cosmic Antiprotons

provide very stringent bounds on DM

Antideuterons

prospects for detection

- NF, Maccione, Vittino
“Dark matter searches with cosmic antideuterons: status and perspective”
arXiv:arXiv:1306.4171 [to appear in JCAP]
- NF, Maccione, Vittino
“Antiproton bounds on dark matter”
In preparation

Radio signal

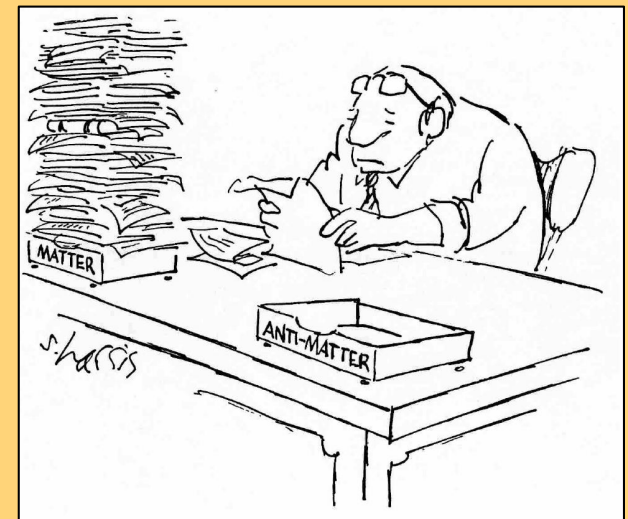
already provide interesting bounds
good prospects for future survey

- NF, Líneros, Regís, Taoso
“A dark matter interpretation for the ARCADE excess?”
Phys. Rev. Lett. 107 (2011) 271302
- NF, Líneros, Regís, Taoso
“Galactic synchrotron emission from WIMPs at radio frequencies”
JCAP 01(2012)005
- NF, Líneros, Regís, Taoso
“Cosmological Radio Emission induced by WIMP Dark Matter”
JCAP 03 (2012) 033

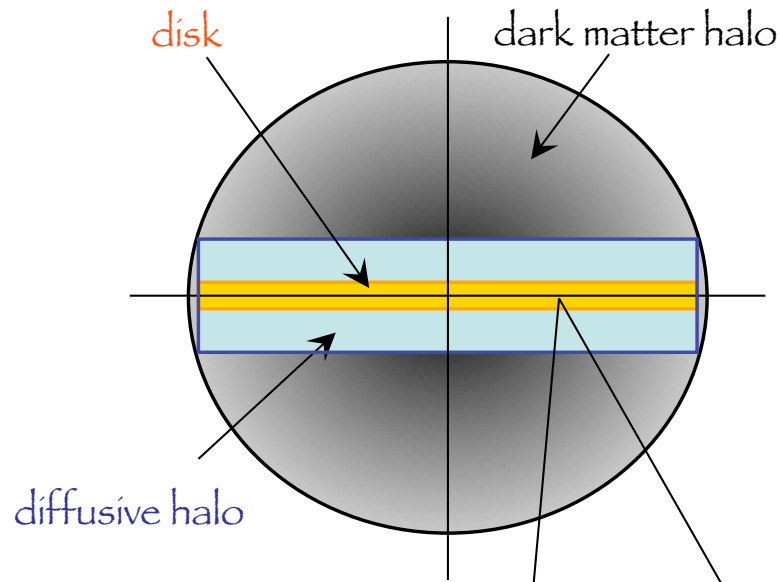
+ some new ideas for DM signal identification

- Camera, Fornasa, NF, Regís
“A novel approach in the WIMP quest: Cross-Correlation of Gamma-Ray Anisotropies and Cosmic Shear”
Ap J Lett 771 (2013) L5
- Camera, Fornasa, NF, Regís
“Redshift tomography and spectral analysis of cosmic shear/gamma-rays anisotropies cross-correlation”
In preparation

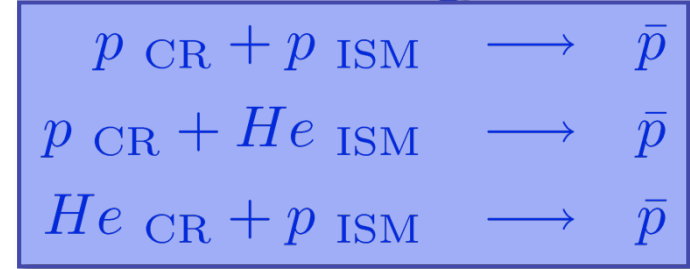
ANTIPROTONS ANTIDEUTERONS



Cosmic antiprotons



Secondaries (background)



Produced in the disk

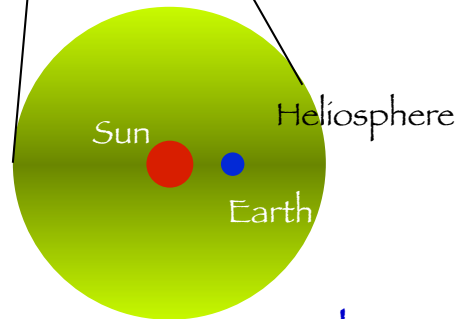
Propagation and energy redistribution in the diffusive halo

DM signal



Produced in the DM halo

Propagation and energy redistribution in the diffusive halo

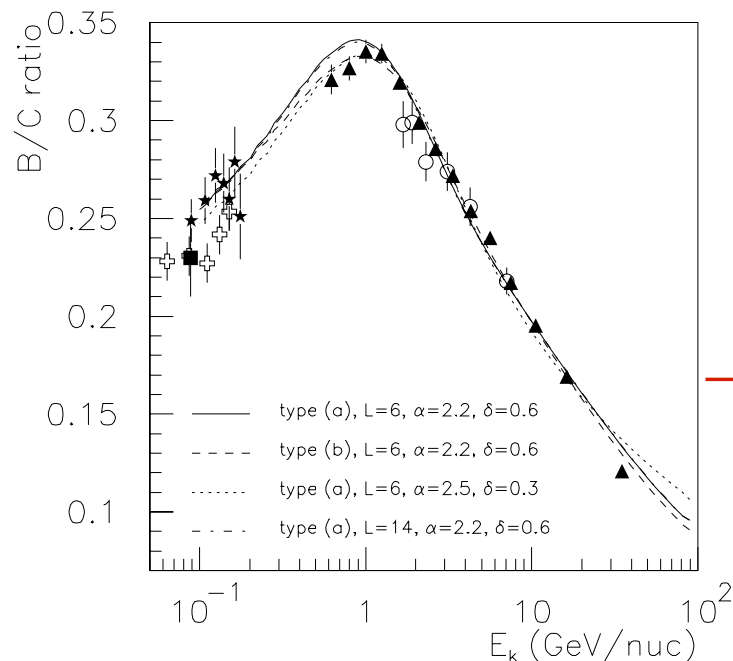


solar modulation

Transport in the galactic medium



Propagation model constrained by secondary/primary ratios, mainly B/C

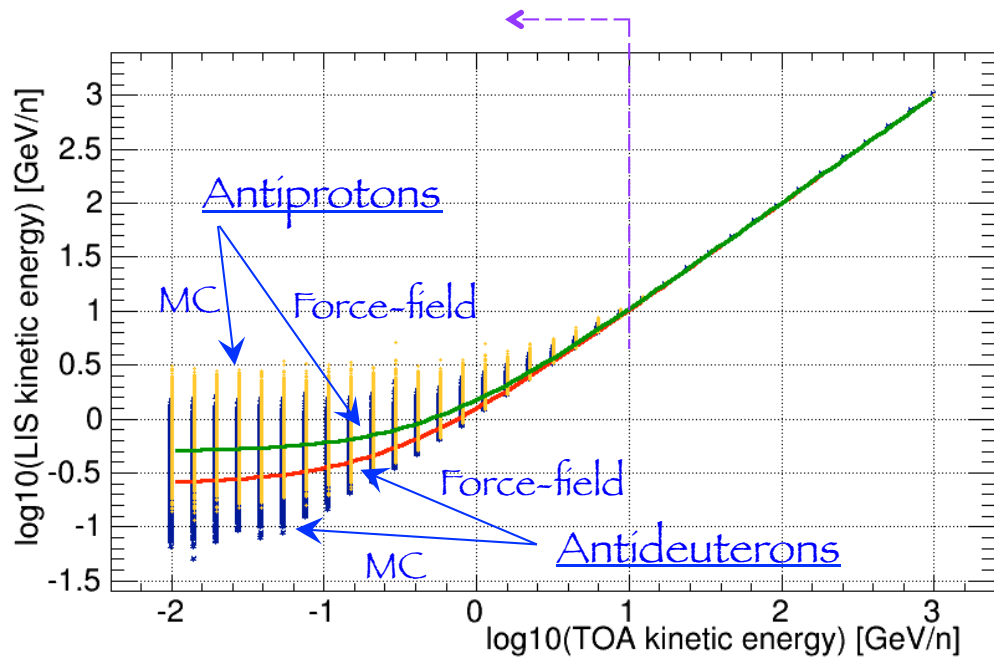


case	diffusion			reacceleration		$\chi_{B/C}^2$
	δ	K_0 (kpc ² /Myr)	L (kpc)	V_c (km/sec)	V_A (km/sec)	
max	0.46	0.0765	15	5	117.6	39.98
med	0.70	0.0112	4	12	52.9	25.68
min	0.85	0.0016	1	13.5	22.4	39.02

convection

+ energy losses, scattering, annihilation

Transport in the heliosphere



CR transport in the heliosphere treated with a “stochastic equation” technique:

- phase space density sampled and evolved according to a random walk set by the diffusion properties of the heliosphere

Model parameters and geometry:

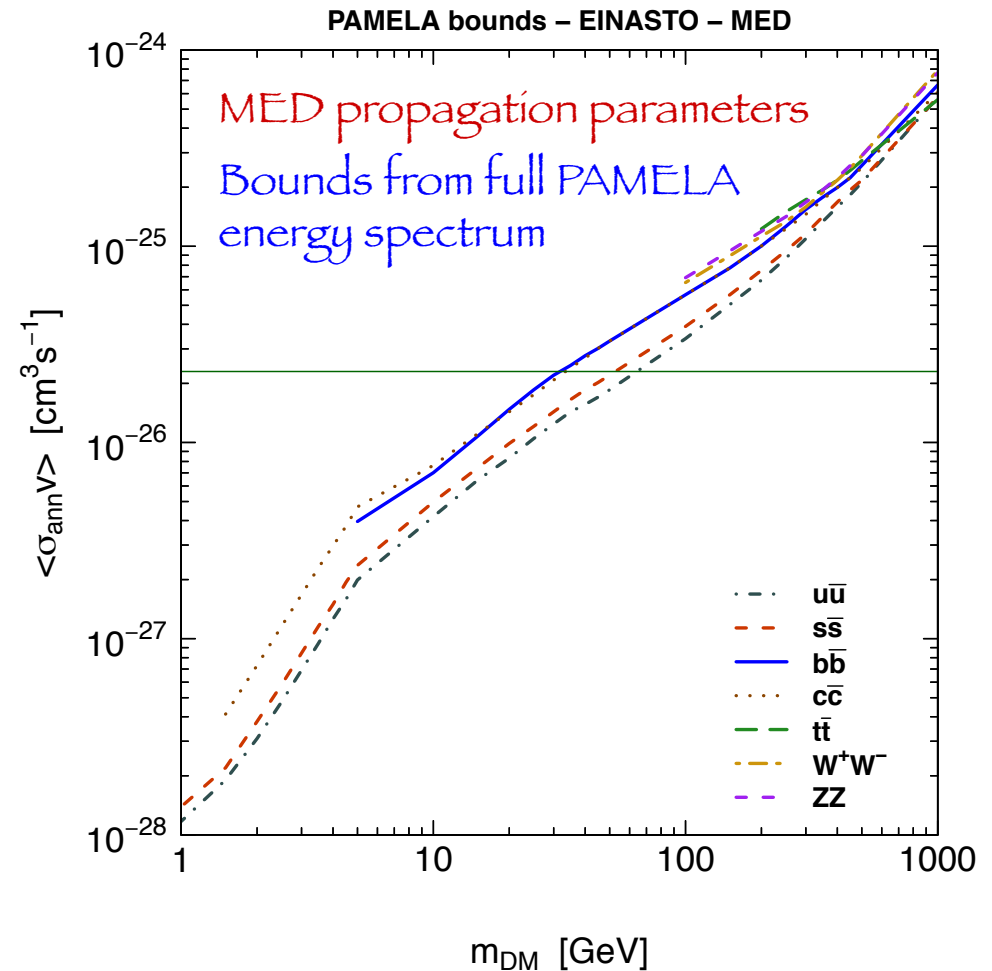
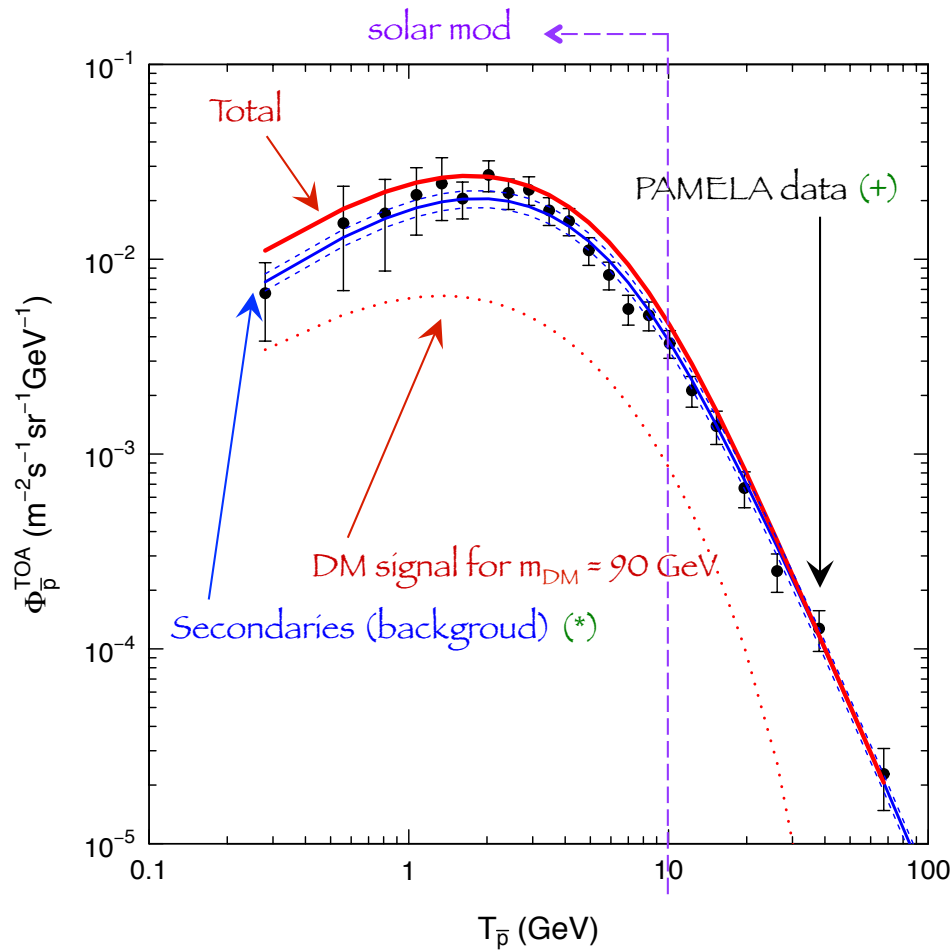
Solar magnetic field: Parker spiral

Tilt angle of the current-sheet α

Mean free path $\lambda_{\parallel} = \lambda_0(\rho/1 \text{ GeV})^{\gamma}(B_{\oplus}/B)$

Polarity (changes every 11 yr)

Antiproton bounds on DM properties

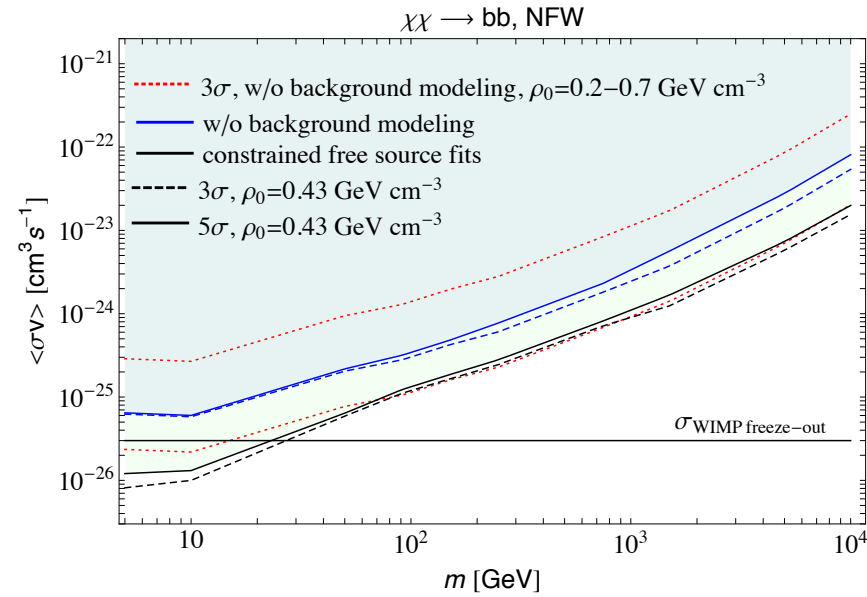
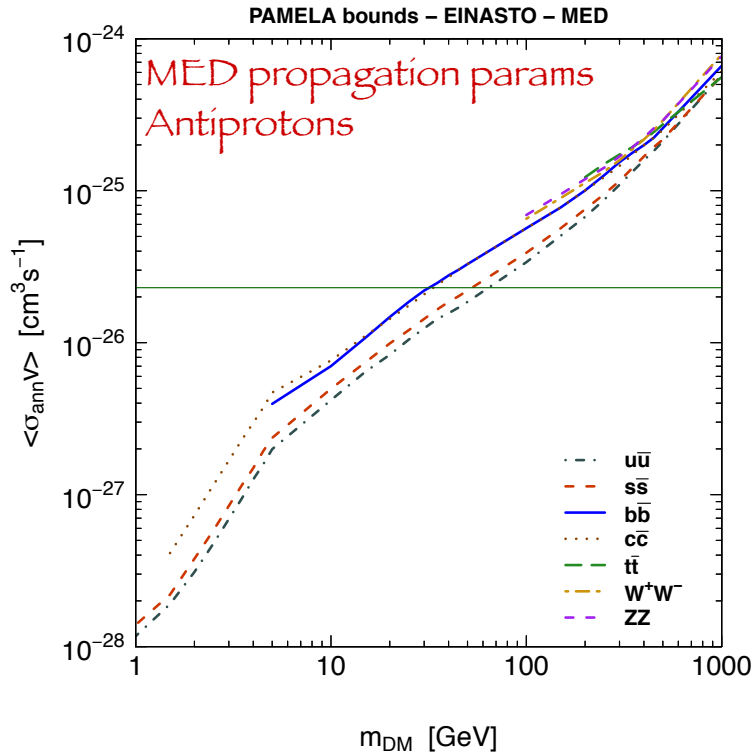


(*) Donato, Maurin, Brun, Delahaye, Salati, PRL 102 (2009) 071301
 (+) Adriani et al. (PAMELA Collab.), PRL 105 (2010) 121101

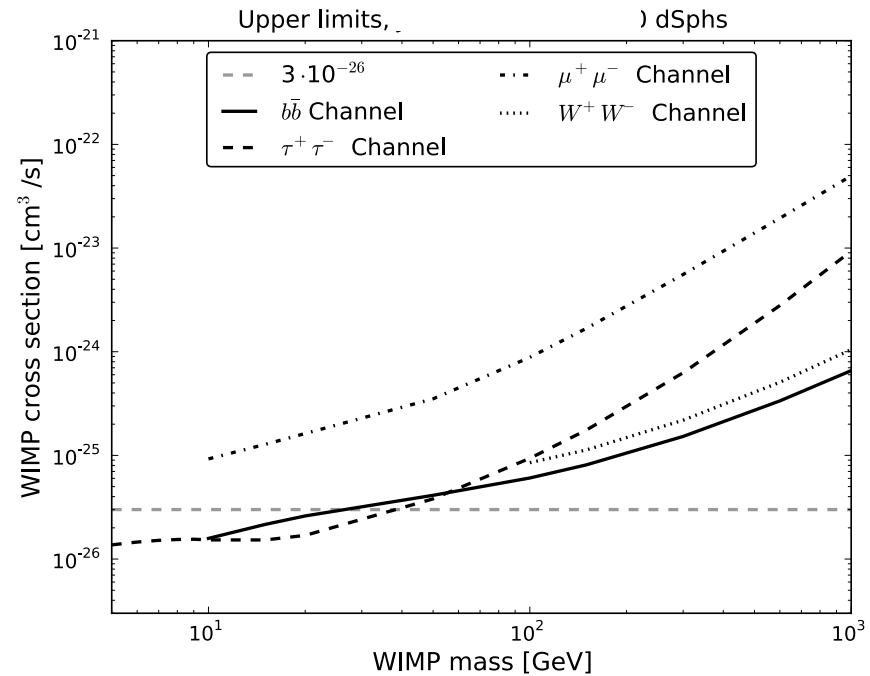
Fornengo, Maccione, Vittino, in preparation

Caveat: the bounds are reported (as is usual) under the hypothesis that the DM candidate is the dominant DM component, regardless of its thermal properties in the early Universe

Comparison with gamma-rays bounds



Fermi analysis on diffuse gamma rays emission

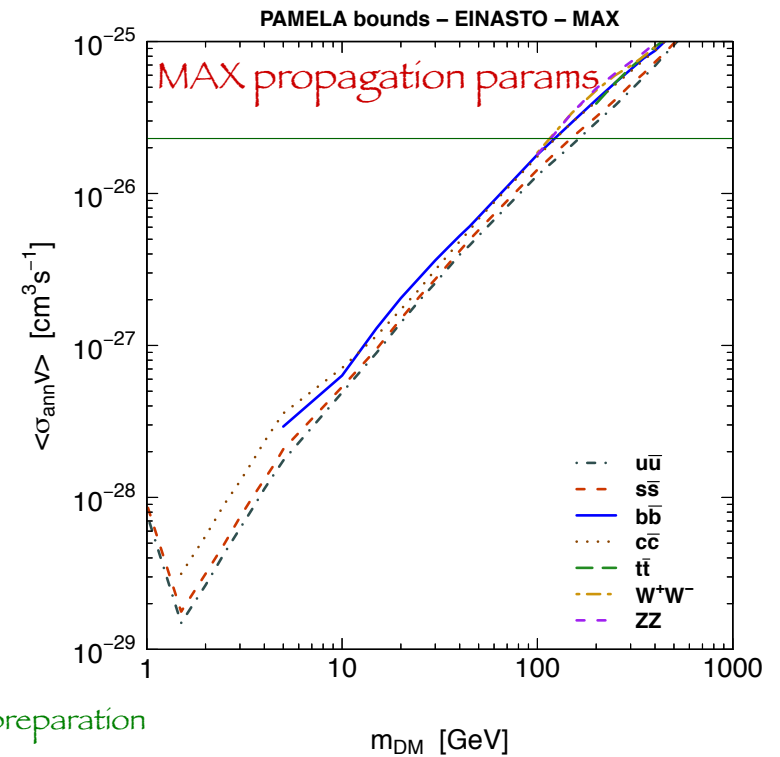
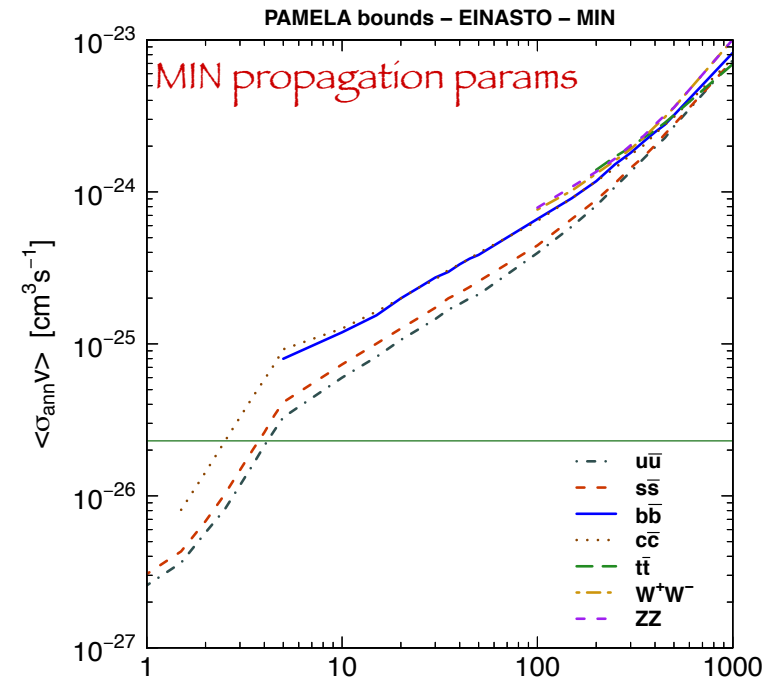
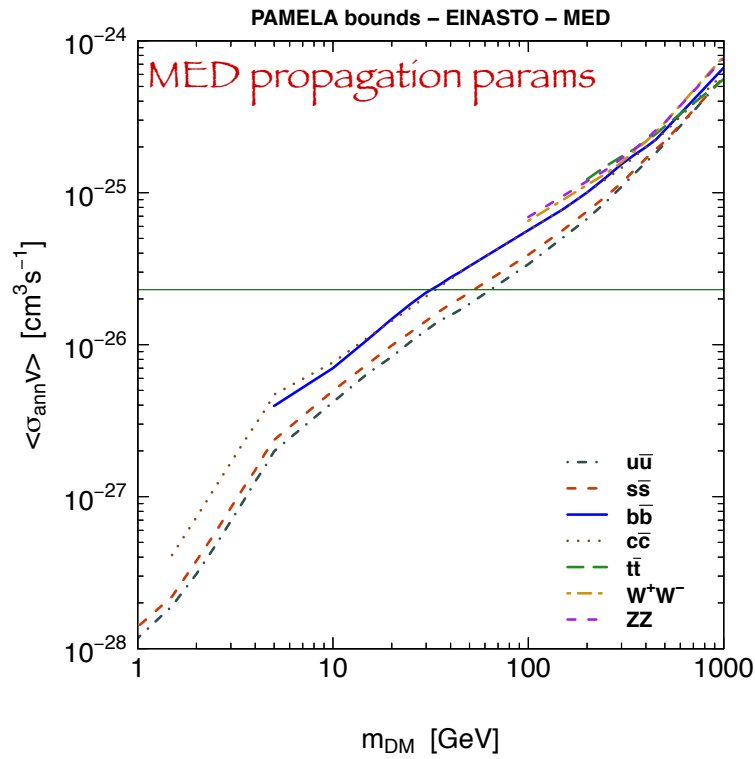


Fermi analysis on dwarf spheroidals

Ackermann et al., *Astrop. J.* 761 (2012) 91
See also: Bringmann et al., arXiv:1307.3284

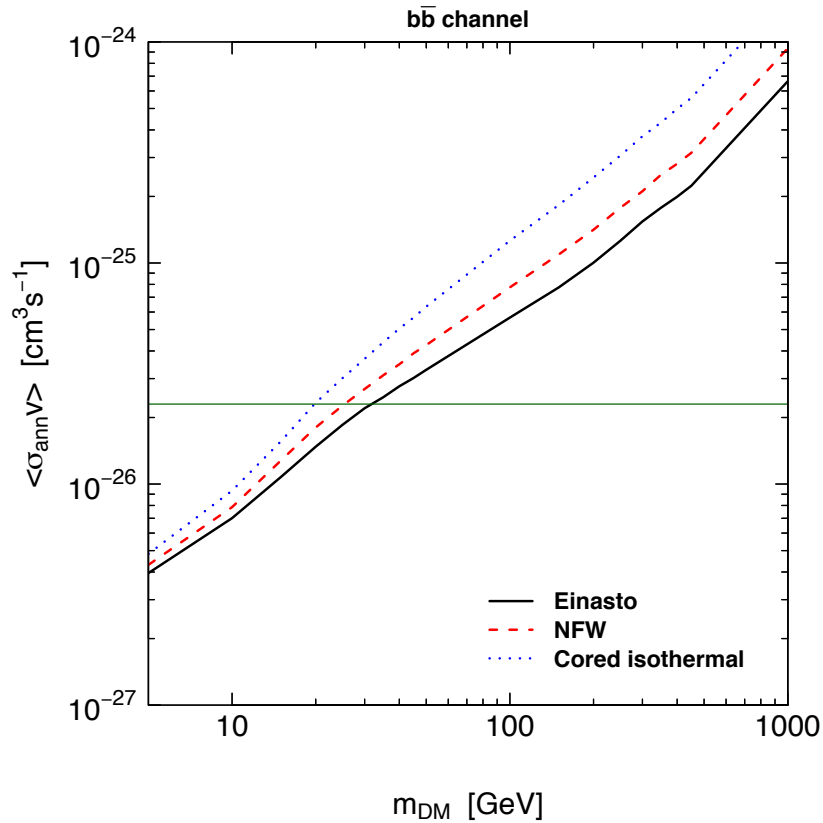
Ackermann et al., *PRL* 107 (2011) 241302
See also: Geringer-Sameth et al. *PRL* 107 (2011) 241303

Antiproton bounds

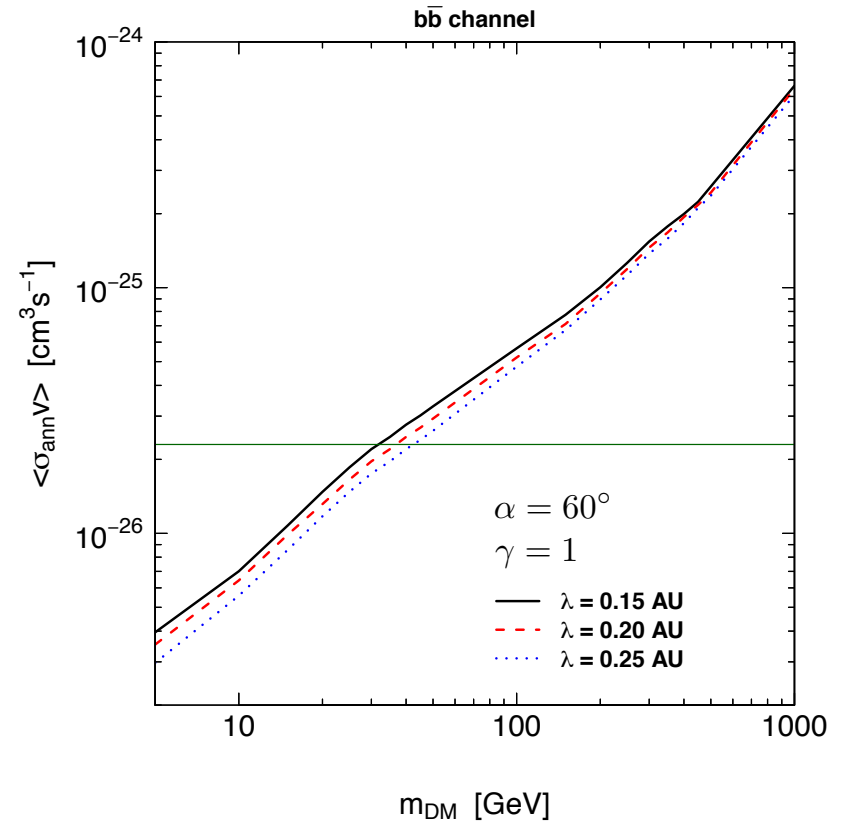


Dependence on modeling of
CR transport in the Galaxy

Antiproton bounds



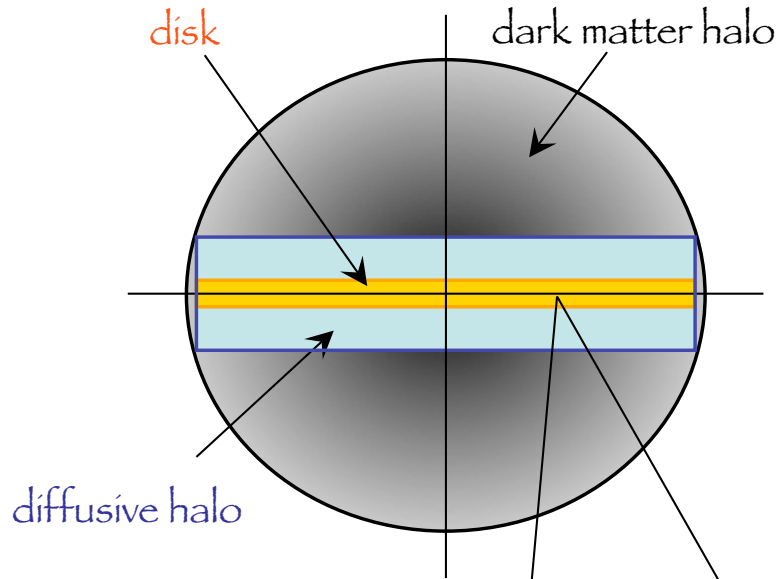
Dependence on the DM halo profile



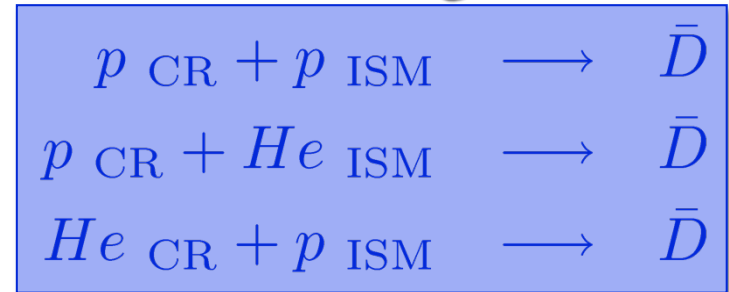
Dependence on solar modulation

Cosmic antideuterons

F. Donato, N. Fornengo, P. Salati, PRD 62 (2000) 043003



Secondaries (background)



Produced in the disk

Propagation and energy redistribution in the diffusive halo

DM signal



Produced in the DM halo

Propagation and energy redistribution in the diffusive halo

solar modulation

Coalescence process

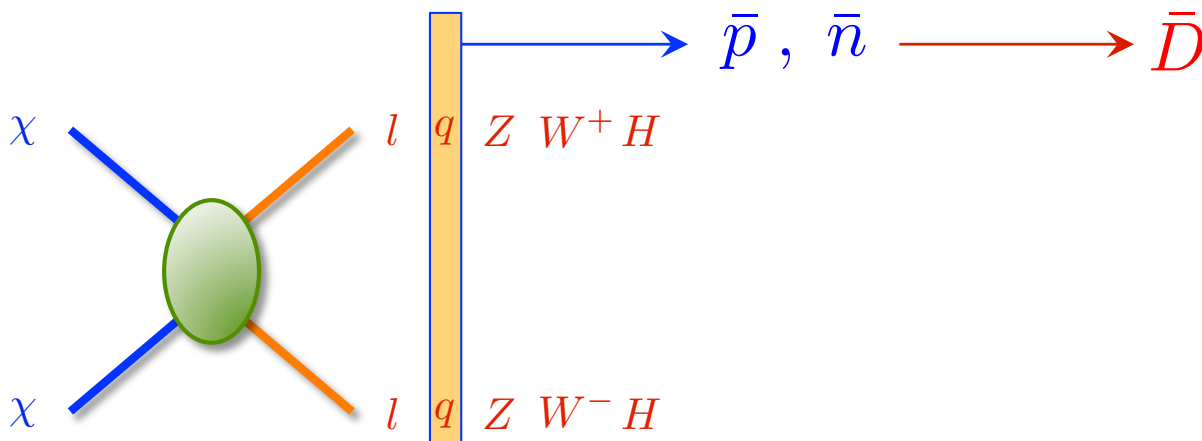
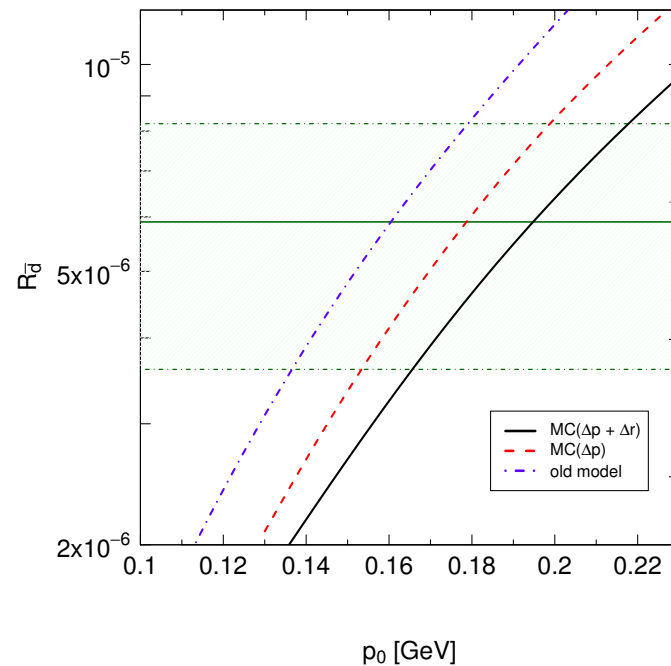
$$\frac{dN_{\bar{d}}}{dT_{\bar{d}}} = (4\pi E_{\bar{d}} k_{\bar{d}}) F_{\bar{d}}^{\text{MC}}(\sqrt{s}, \vec{k}_{\bar{d}})$$

$$F_{\bar{d}}^{\text{MC}}(\sqrt{s}, \vec{k}_{\bar{d}}) = \int F_{(\bar{p}\bar{n})}^{\text{MC}}(\sqrt{s}, \vec{k}_{\bar{p}}, \vec{k}_{\bar{n}}) C(\Delta) \delta^3(\vec{k}_{\bar{d}} - \vec{k}_{\bar{p}} - \vec{k}_{\bar{n}}) d^3\vec{k}_{\bar{n}} d^3\vec{k}_{\bar{p}}$$

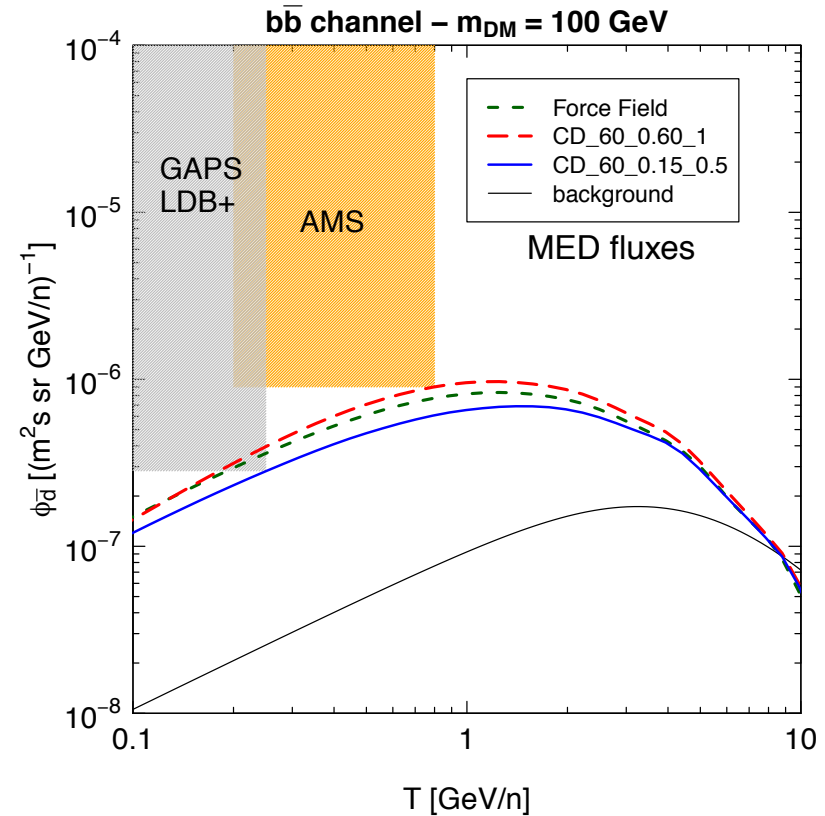
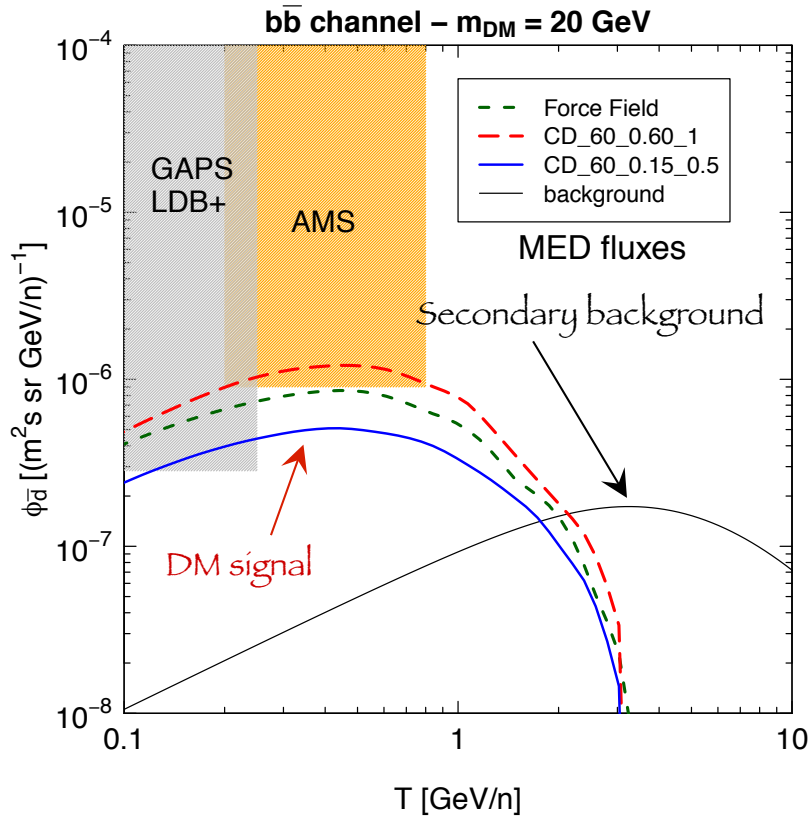
coalescence function

- $\Delta p \leq p_0$ *coalescence momentum*
 - $\Delta r \leq R_{\star}$ *antideuteron radius*
- Fixed on ALEPH data on antiD production

$p_0 = (195 \pm 22) \text{ MeV}$



Detection prospects



DM configurations allowed by antiproton bounds

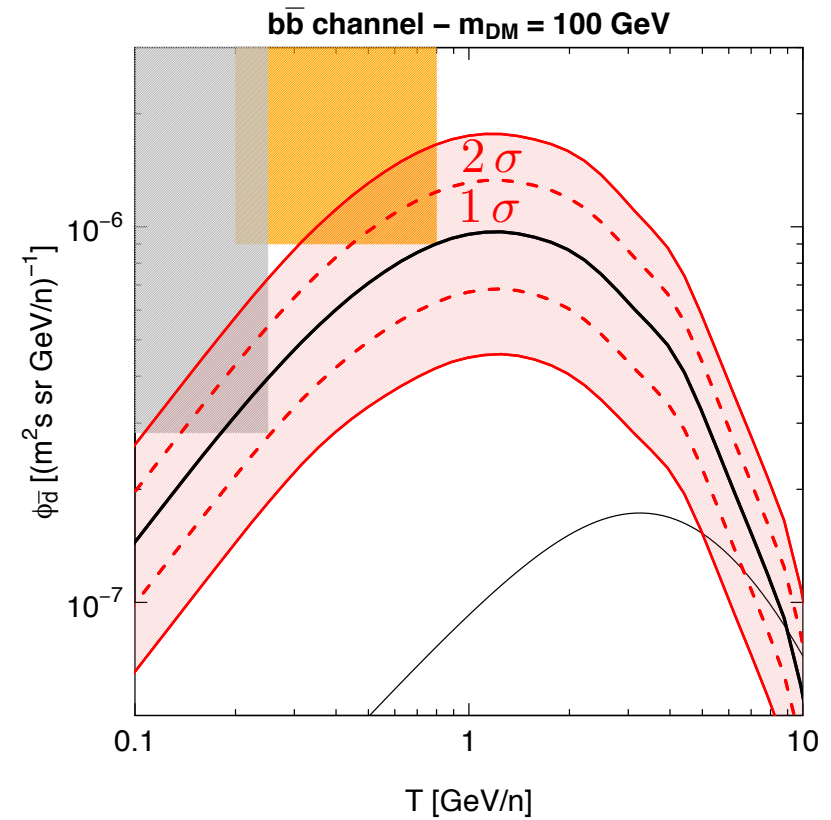
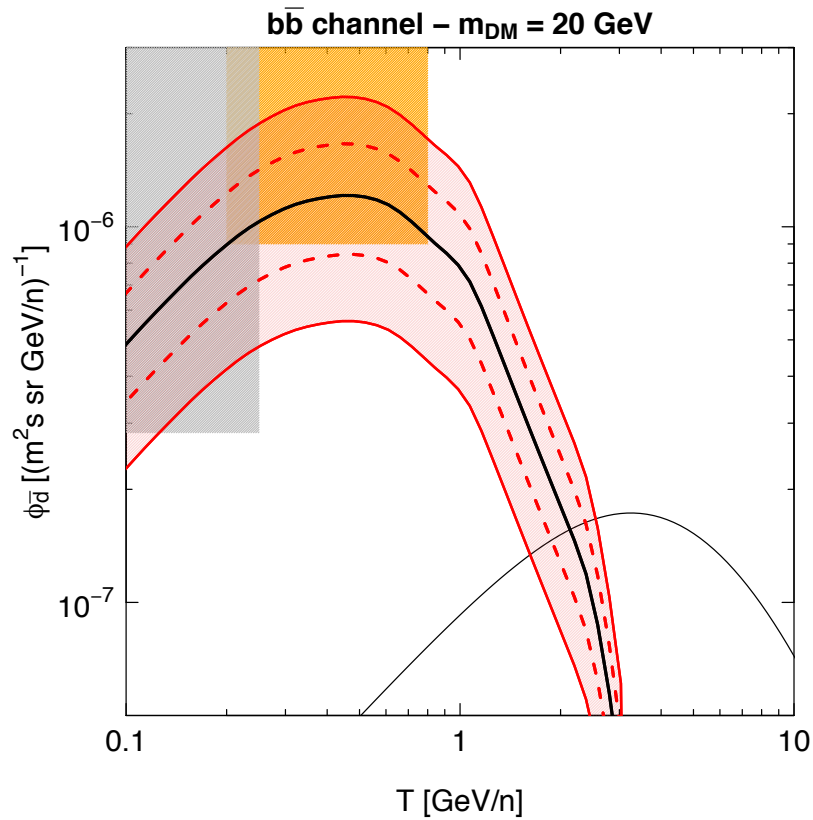
Relevant detection prospects for $D\bar{a}$ energies below few GeV/n, where dependence on solar modulation modeling can have an impact on the DM signal up to a factor of 2

Experimental expected sensitivities : 3σ C.L.

GAPS LDB+ : 1 detected event

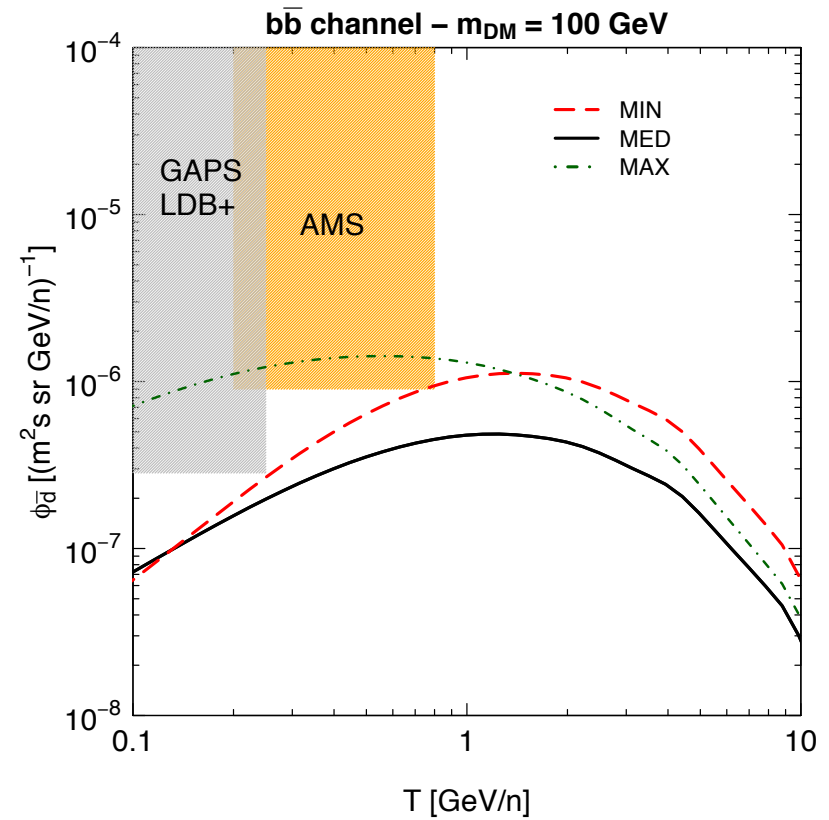
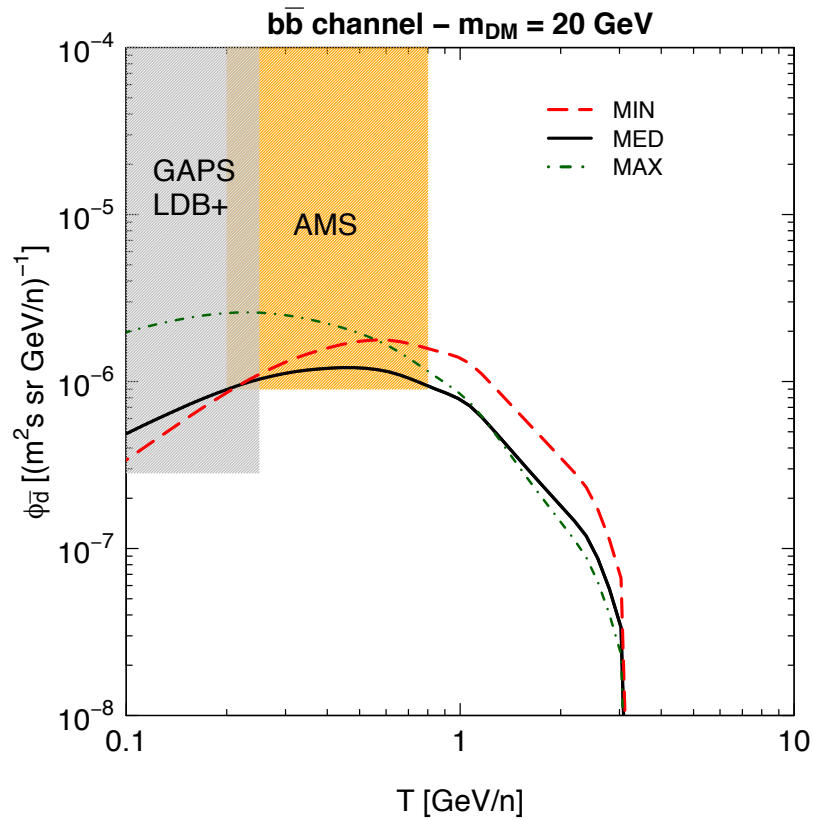
AMS : 2 detected events

Dependence on coalescence momentum

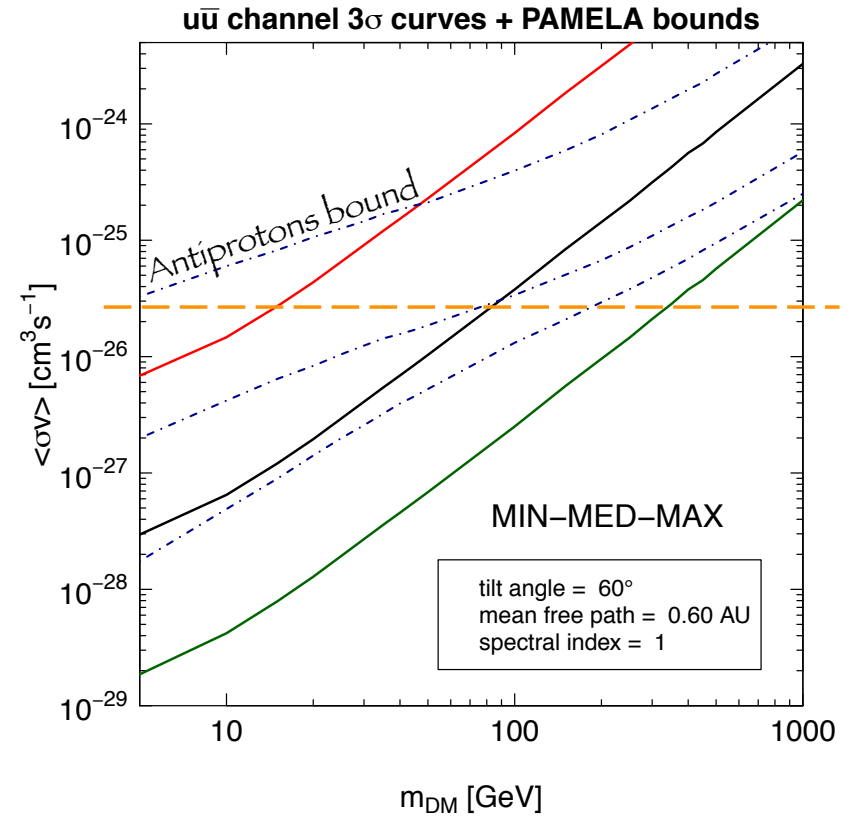
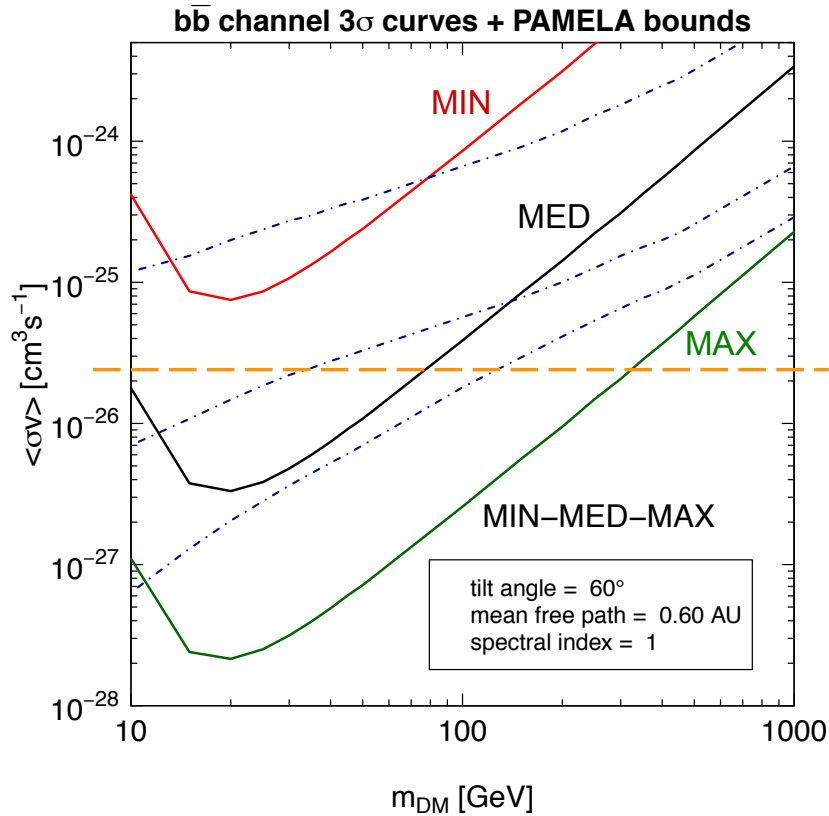


$$p_0 = (195 \pm 22) \text{ MeV}$$

Dependence on galactic transport

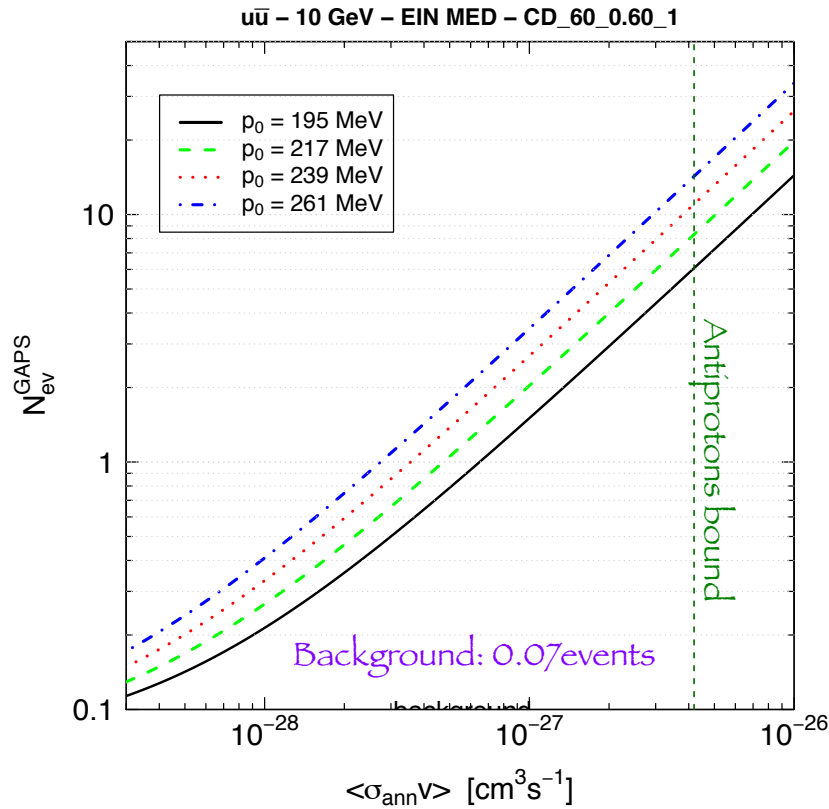


Detection reachability at 3σ C.L.

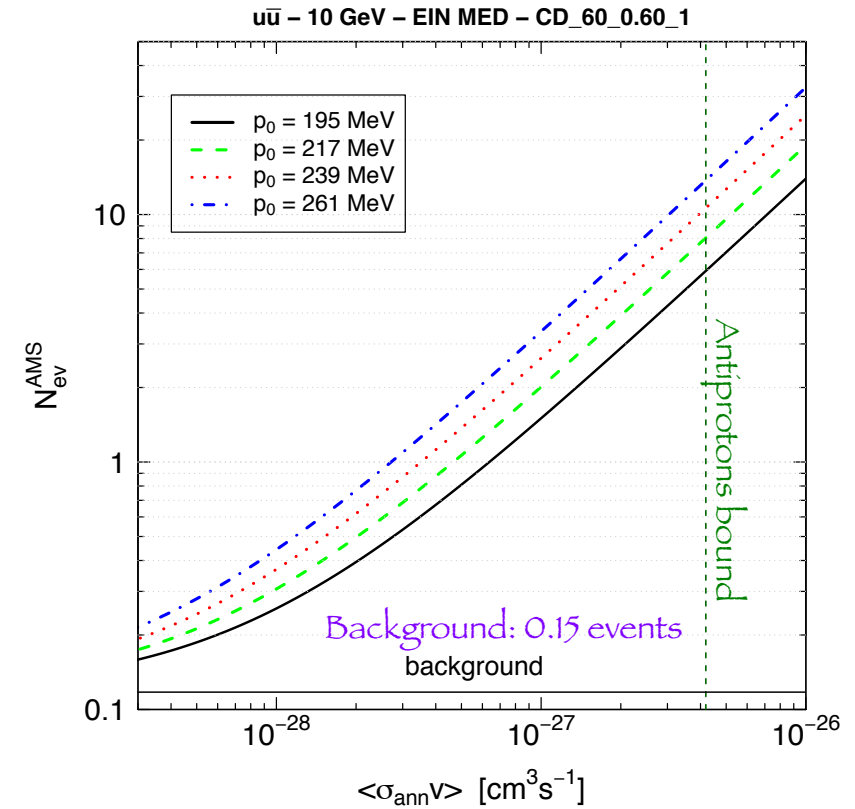


Example for GAPS LDB+ setup
 3σ detection : $N_{crit} \approx 1$ events

Events expected in GAPS and AMS



For GAPS LDB+ setup



For AMS nominal sensitivity

RADIO SIGNALS



Radio signals from dark matter

- DM annihilation (or decay) into e^+/e^- produces radio signals by *synchrotron emission* in galactic/extragalactic *magnetic fields*
- Emission in the *MHz-GHz* frequency range occurs for:
 - Electrons/positrons energies in the *GeV-TeV* range (*)
 - Magnetic fields of the order of *microG*

$$\nu_{\text{GHz}} \sim B_{\mu\text{G}} \left(\frac{E}{15 \text{ GeV}} \right)^2$$

(*) Relevant interval for *WIMP DM* in the *GeV-TeV* mass range

- More specifically: electron energies $< 10 \text{ GeV}$ produce signals at frequencies $< \text{GHz}$

Targets

● Galactic Center

- Good target for spiky DM profiles
- On the scale of the bulge: “WMAP haze” ?
- GC is a very active region: disentanglement of a signal rather complicated

● Galactic Halo

- Mid/high latitudes may be cleaner
- Low radio frequencies for soft e^+/e^- spectra, microwave range otherwise

● Extragalactic diffuse emission

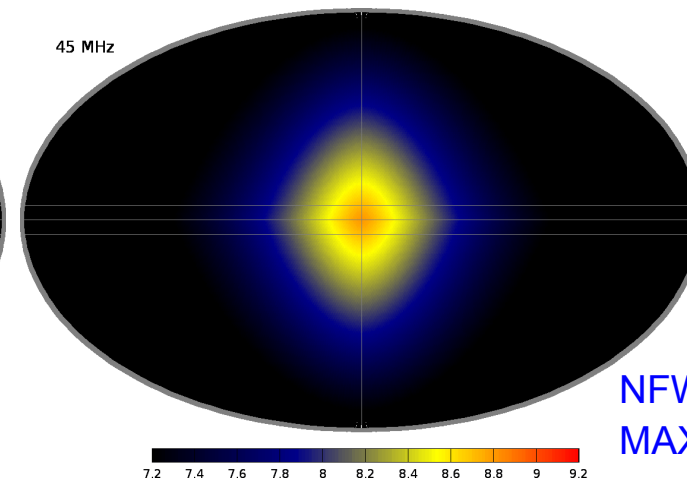
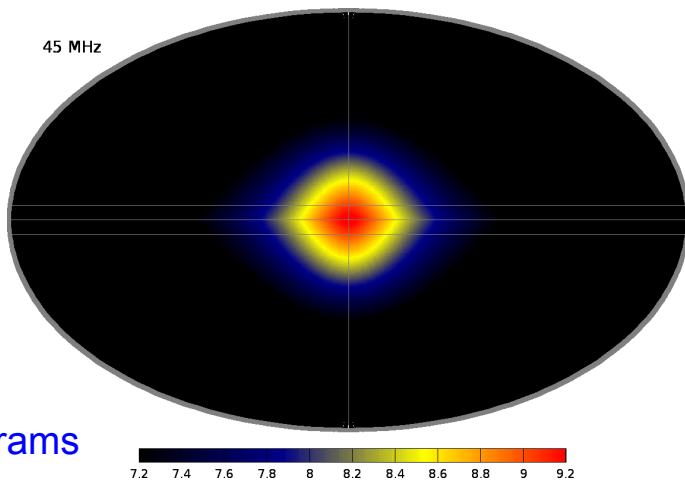
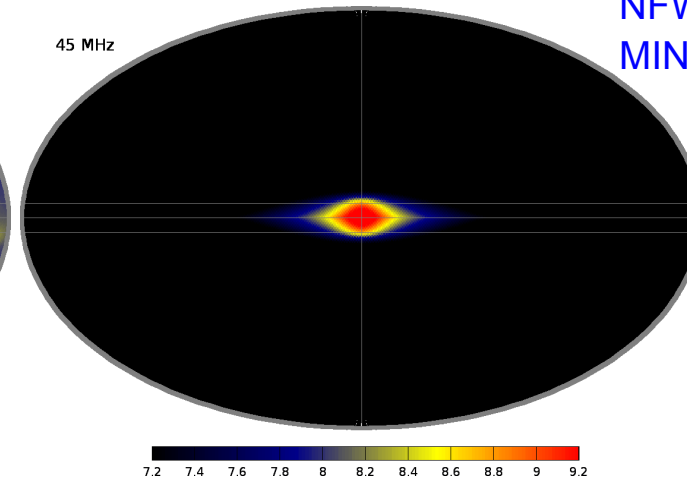
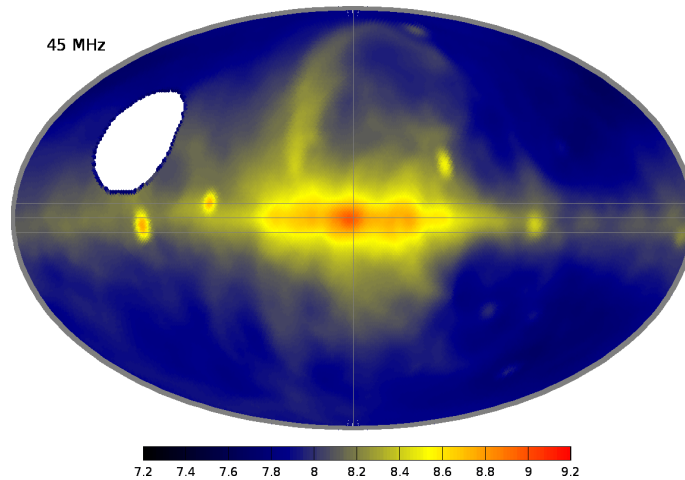
- ARCADE 2: isotropic radio emission significantly brighter than expected: requires a “new” population of unresolved sources which become the most numerous at very low (observationally unreached) brightness [maybe DM ?]
- Anisotropies studies may be a goal for the future

● Extragalactic objects

- Non-thermal emission with spherical morphology correlated with the DM halo profile inferred from kinematic measurements in the external part of extragalactic objects can be a strong indication for WIMP-induced emission
- Promising targets: dwarf spheroidal galaxies and galaxy clusters

Galactic DM: morphology of radio sky at 45 MHz

observed



Forrenigo, Lineros, Regis, Taoso, JCAP 01 (2012) 005

NFW
MED propag params

NFW
MAX propag params

10 GeV DM
Annihilation into muon with thermal cross section
Exp decaying $B(r,z)$ with $B_{TOT} = 6$ microG (GMF I)

NFW tuned to Via Lactea II
No substructures included (checked that are not relevant at $|b| < 30$ deg because of antibiased clump distribution)

Galactic radio signal

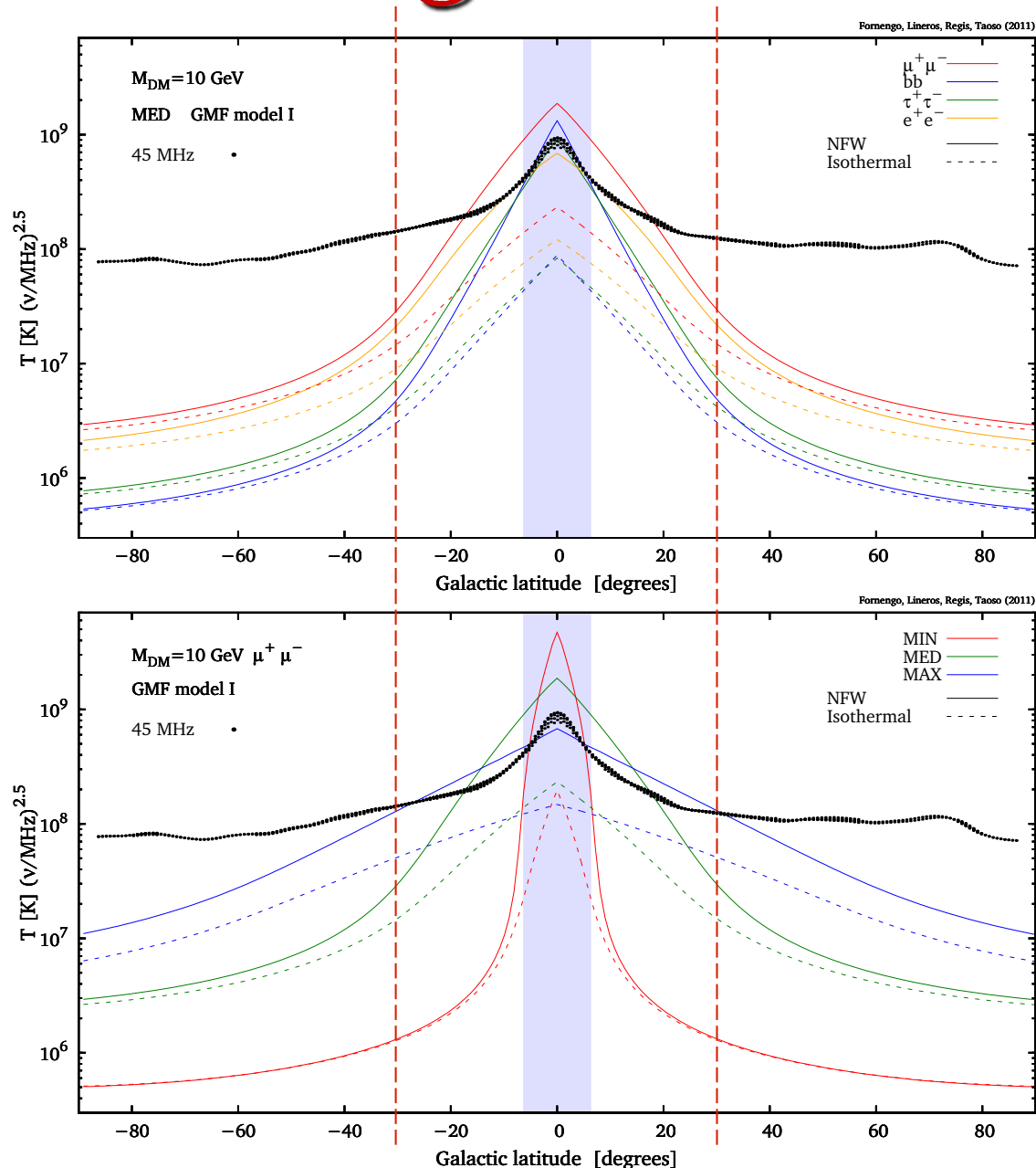
45 MHz

Data: $||l|| < 3^\circ$

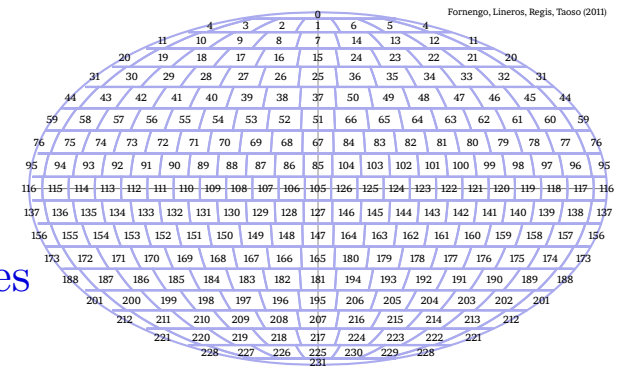
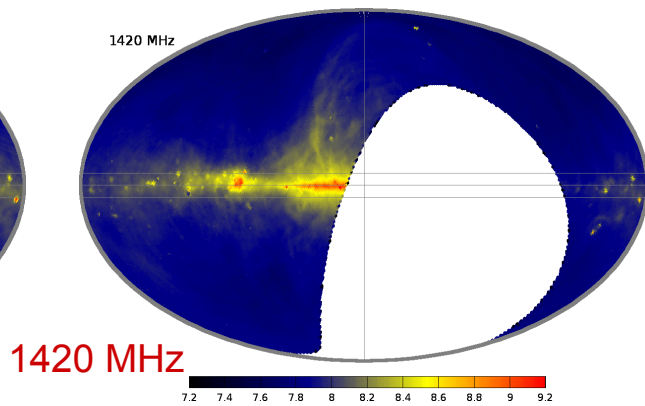
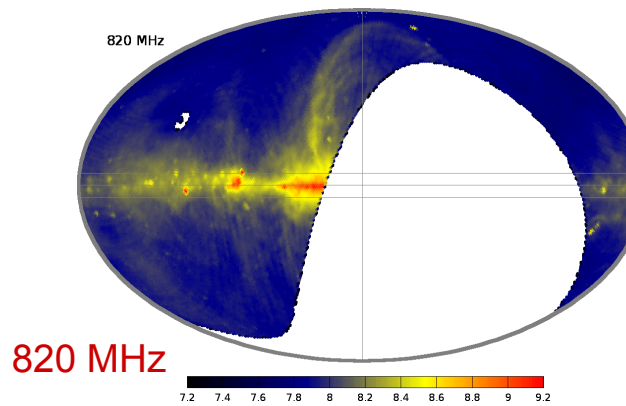
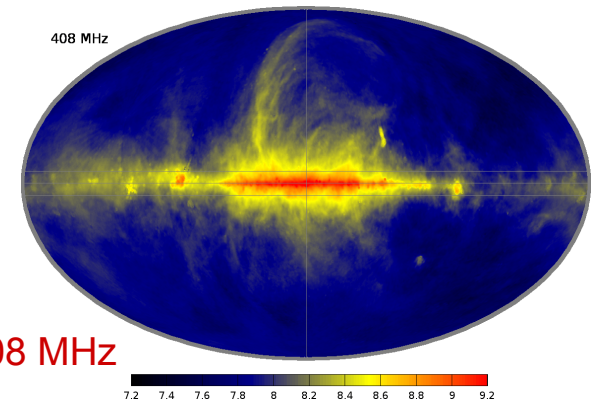
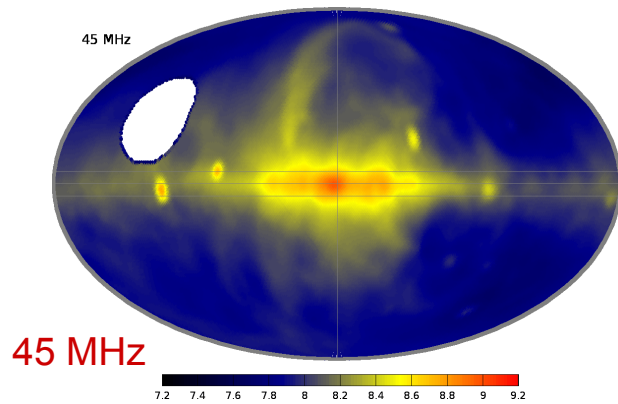
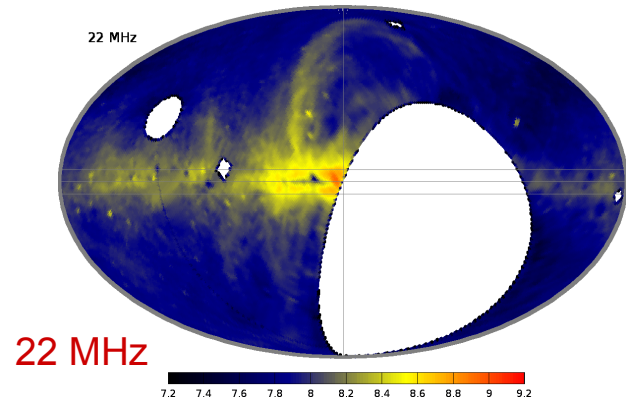
DM models: $l = 0^\circ$

DM could substantially contribute to the radio flux

MED, MAX: allow to search for DM outside the GC region (while form MIN is too concentrated)



Skymaps



$$(T_{\text{obs}})^i \quad i = \text{patches}$$

Galactic radio signal: bounds

Bounds from combination of all frequency skymaps

$$(T_{\text{DM}})^i \leq (T_{\text{obs}})^i + 3\sigma$$

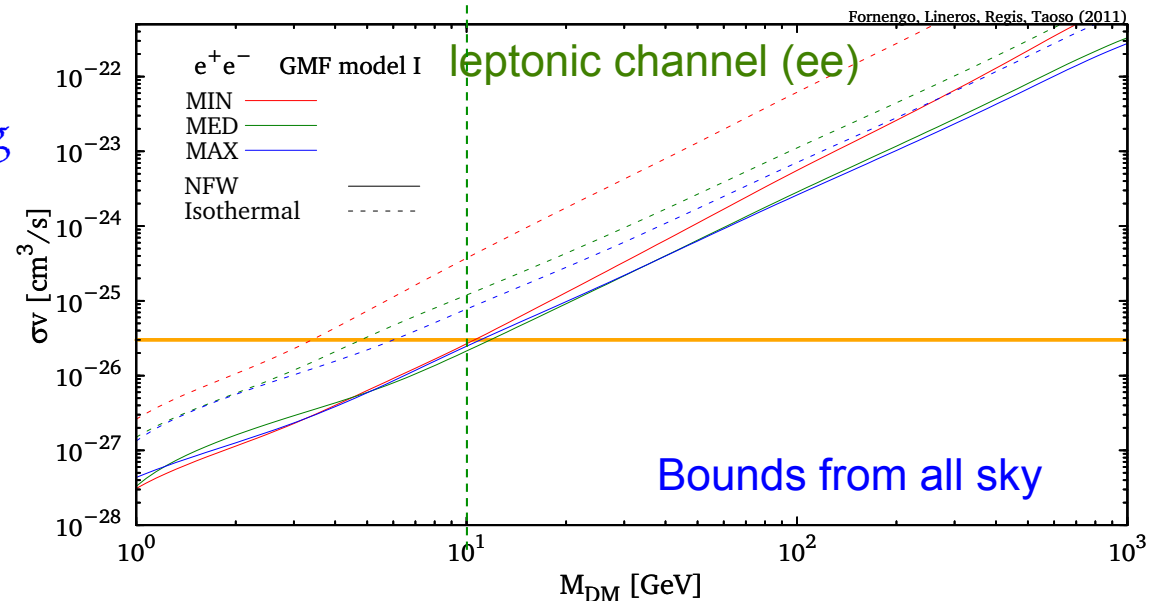
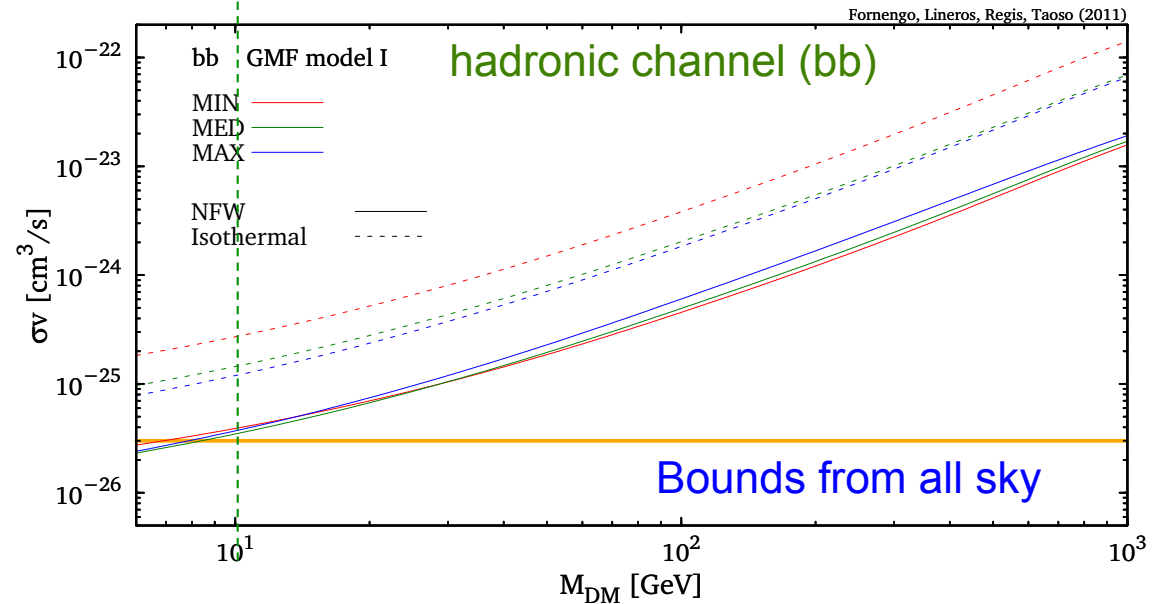
$$[\langle\sigma v\rangle, M_{\text{DM}}] \longleftrightarrow \min_i \{(T_{\text{DM}})^i\}$$

Conservative bounds:

- no astrophysical background subtraction
- no DM substructures included (*)

No strong dependence of bound on magnetic field because most constraining patches are those at low latitude, where various $B(r,z)$ do not sizeably differ

ν [MHz]	Survey	rms noise [K]
22	DRAO	5000
45	Guzman et al.	3500
408	Haslam et al.	0.8
820	Dwingeloo	1.4
1420	Stockert	0.02

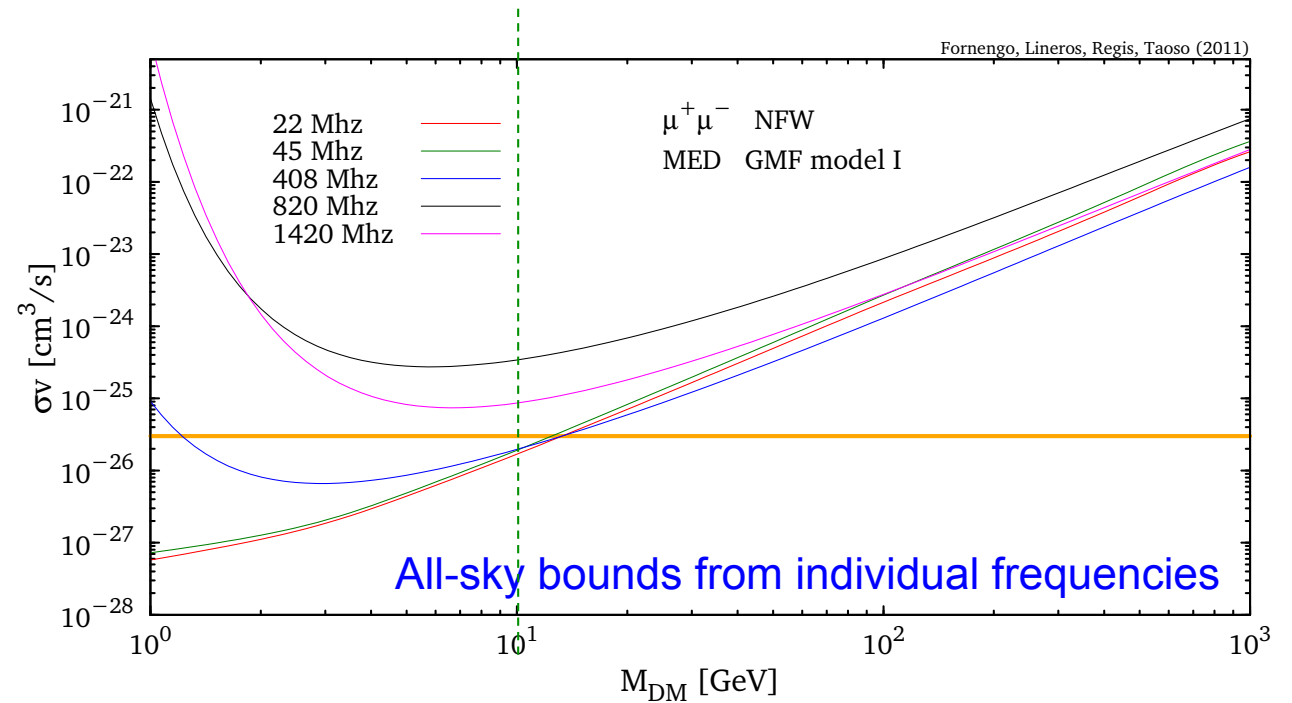


Fornengo, Líneros, Regis, Taoso, JCAP 01 (2012) 005 [arXiv:1110.4337]

(*) See: Borriello, Cuoco, Miele, PRD 79 (2009) 023518

Galactic radio signal: bounds

ν [MHz]	Survey	rms noise [K]
22	DRAO	5000
45	Guzman et al.	3500
408	Haslam et al.	0.8
820	Dwingeloo	1.4
1420	Stockert	0.02



Lower frequencies better for lighter DM

Constraining power also depends on sky-coverage and sensitivity of the survey

Extragalactic signal

- Radio emission may occur also in extragalactic halos
- Three relevant observables:
 - Intensity of the emission
 - High frequency: CMB largely dominates
 - Close and below 1 GHz: CMB may be efficiently subtracted
 - Low frequencies: extra-galactic sources dominate
 - Differential number counts of sources
 - Quite useful to study different radio populations
 - Dominated by radio-loud AGNs down to the mJy level
 - Star-forming galaxies and radio-quiet AGN take over at fainter fluxes
 - Angular correlations
 - Angular distribution of sources is a powerful probe of LS clustering
 - Wide-area radio surveys allow to test large scales
 - 2-point correlation function and angular power spectrum

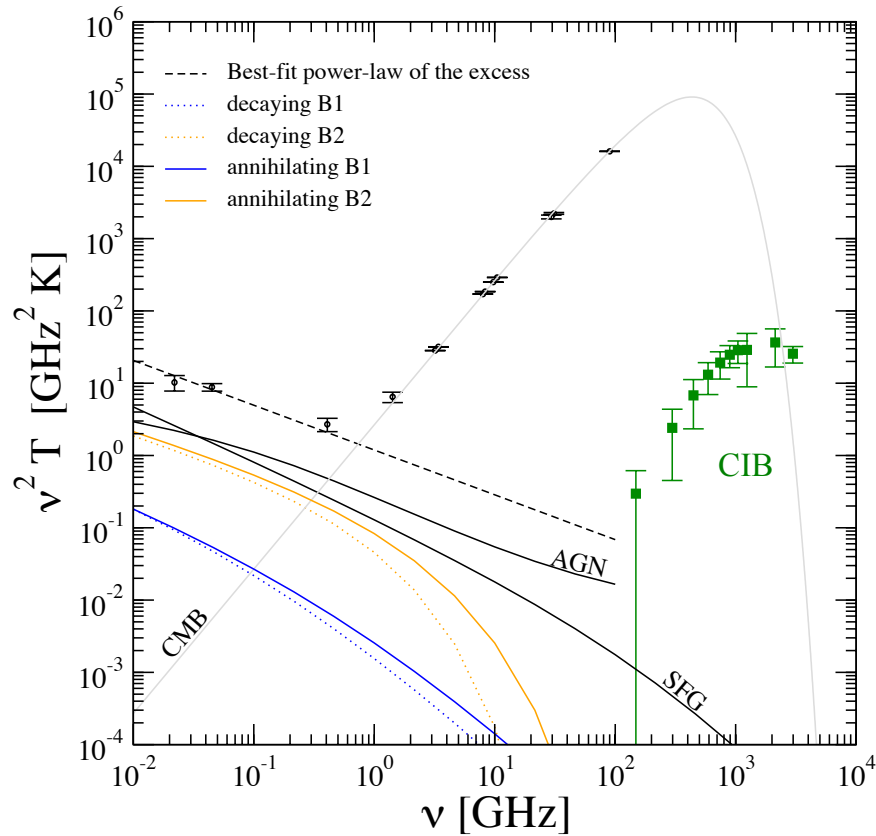
Extragalactic signal

Key elements:

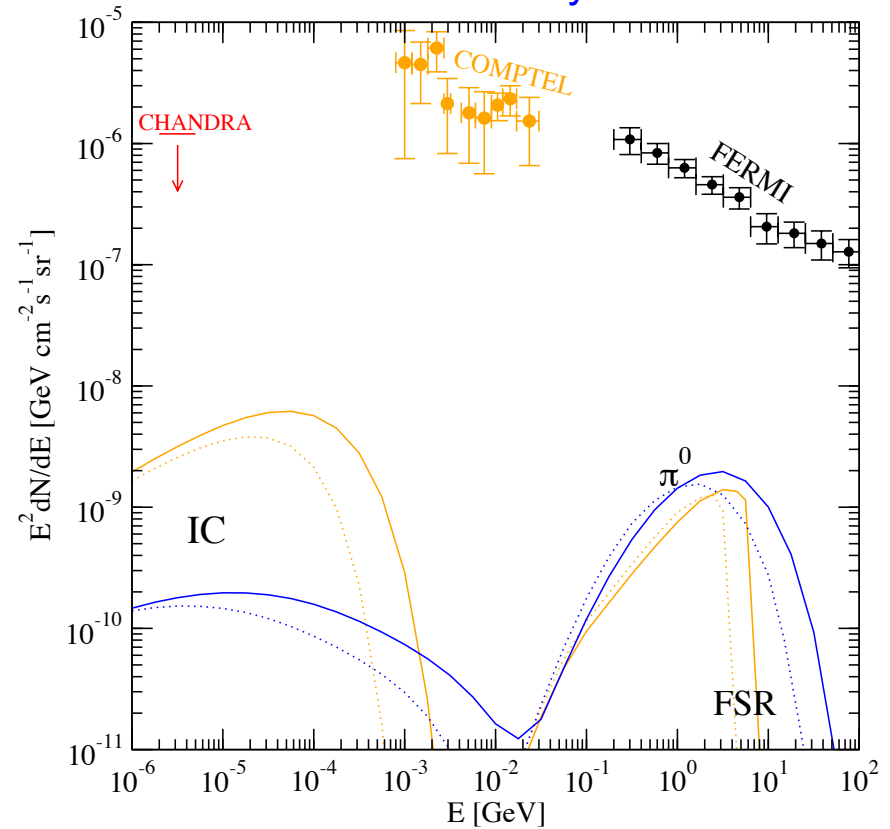
- Halo mass function and concentration
- DM distribution in halos
- Cosmological evolution
- e^+/e^- propagation and energy losses
- Magnetic fields

Total intensity

Radio



Gamma-rays



Radio is quite constraining for DM producing leptons

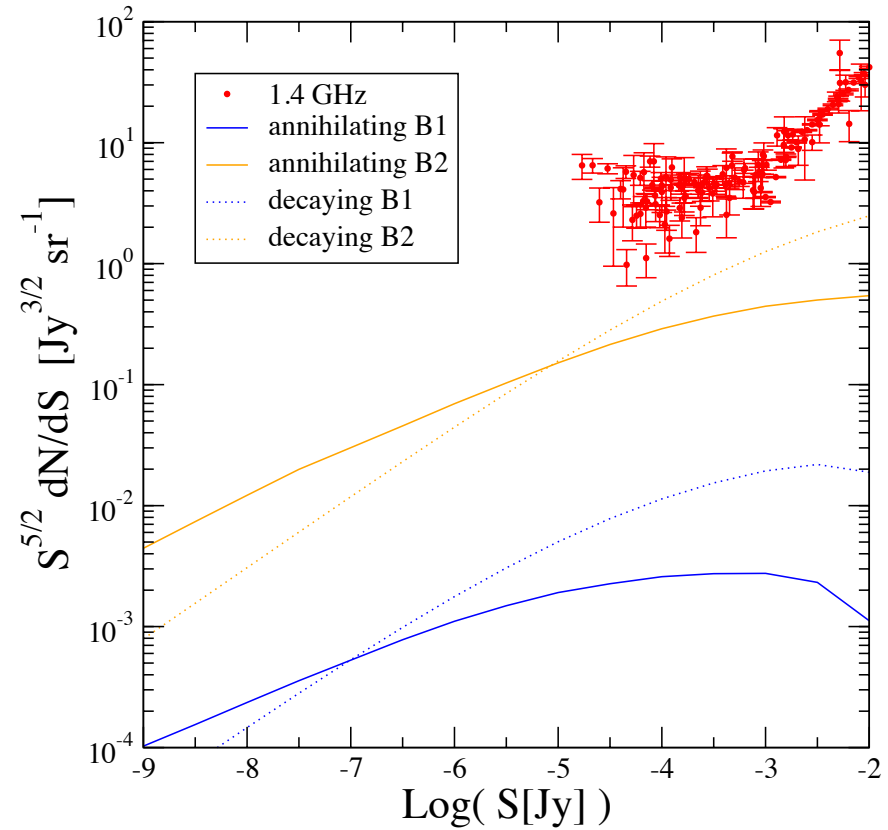
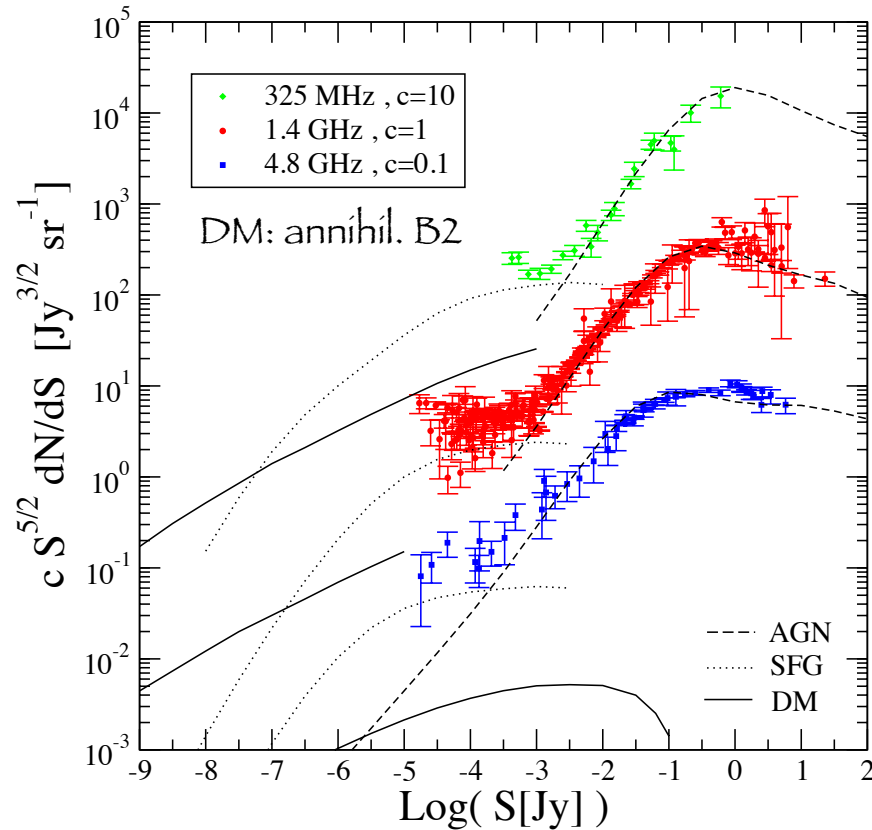
For DM producing hadrons, constraining power is “similar” to gamma-rays

Illustrative benchmarks

Name	Mass [GeV]	$(\sigma_a v)$ [cm ³ s ⁻¹] annihilating case	τ [s] decaying case	Dominant final state
B1	100	$3 \cdot 10^{-26}$	$4 \cdot 10^{28}$	$b - b$
B2	10	$3 \cdot 10^{-26}$	$5 \cdot 10^{27}$	$\mu^+ - \mu^-$

Source number counts

Benchmark B2

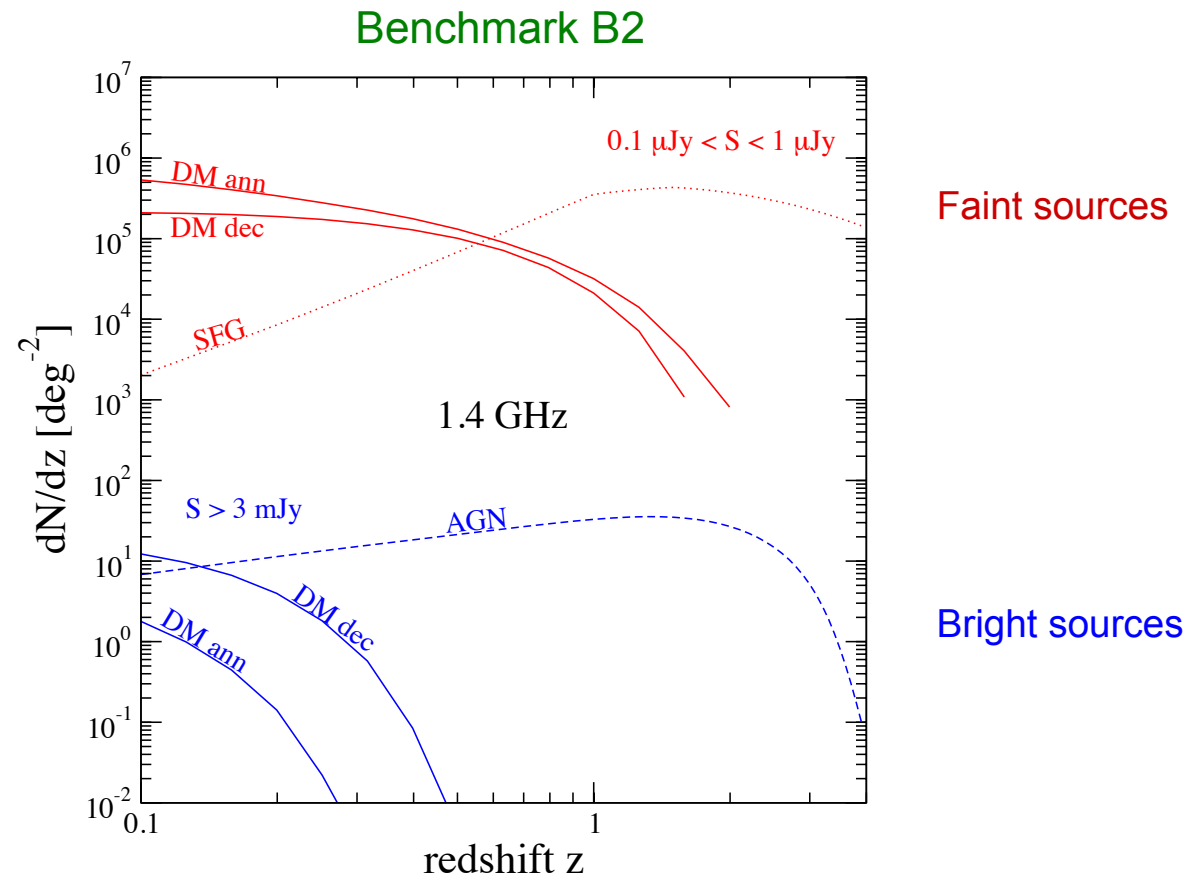


DM contribution becomes more dominant at sub-microJy levels

Decaying-DM spectrum steeper \rightarrow takes over at even smaller fluxes

Annihilating DM(density)²+ (growing of concentration at small halo masses): makes the smaller and fainter structures more important than brighter halos

Differential number counts

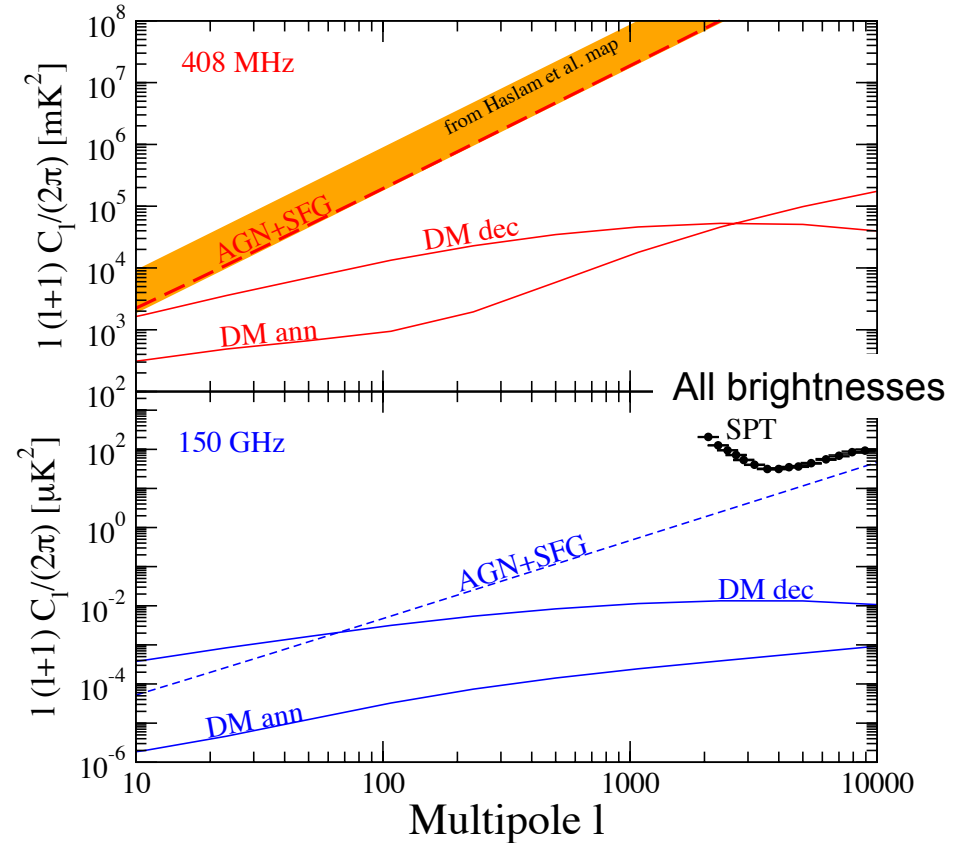
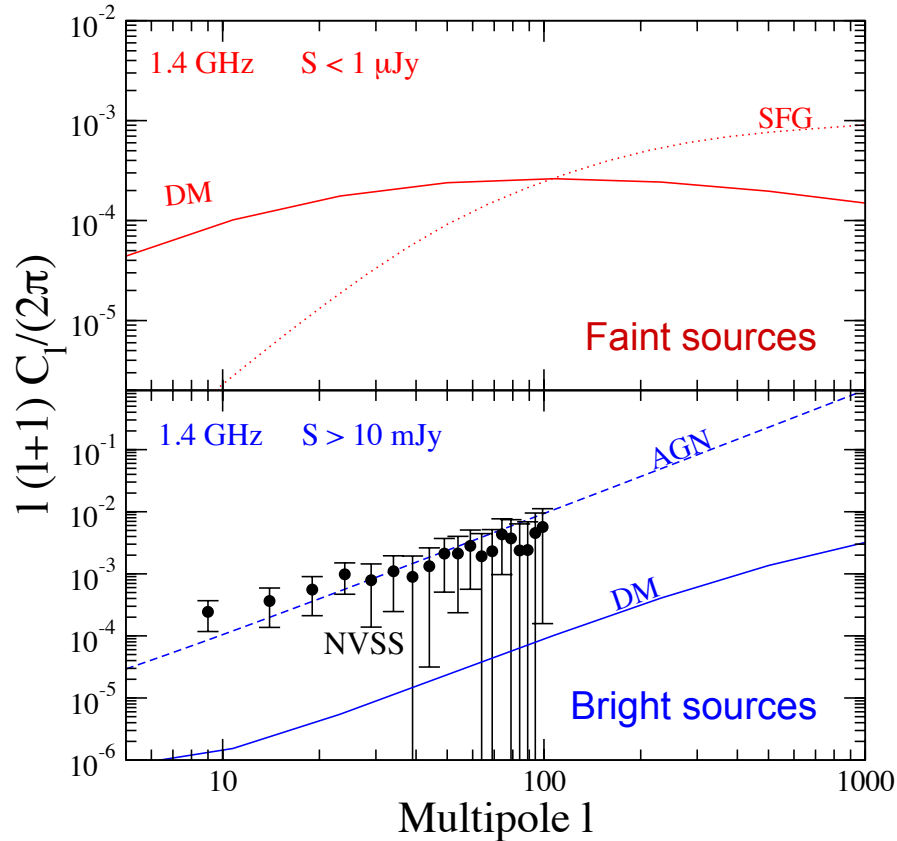


DM-induced radio emission is mostly produced at low-redshifts

DM pop able to give sizeable contrib to total intensity has to dominate source counts at low brightness ($S < 1 \mu\text{Jy}$) and low z ($z < 1$)

Angular correlation

Benchmark B2

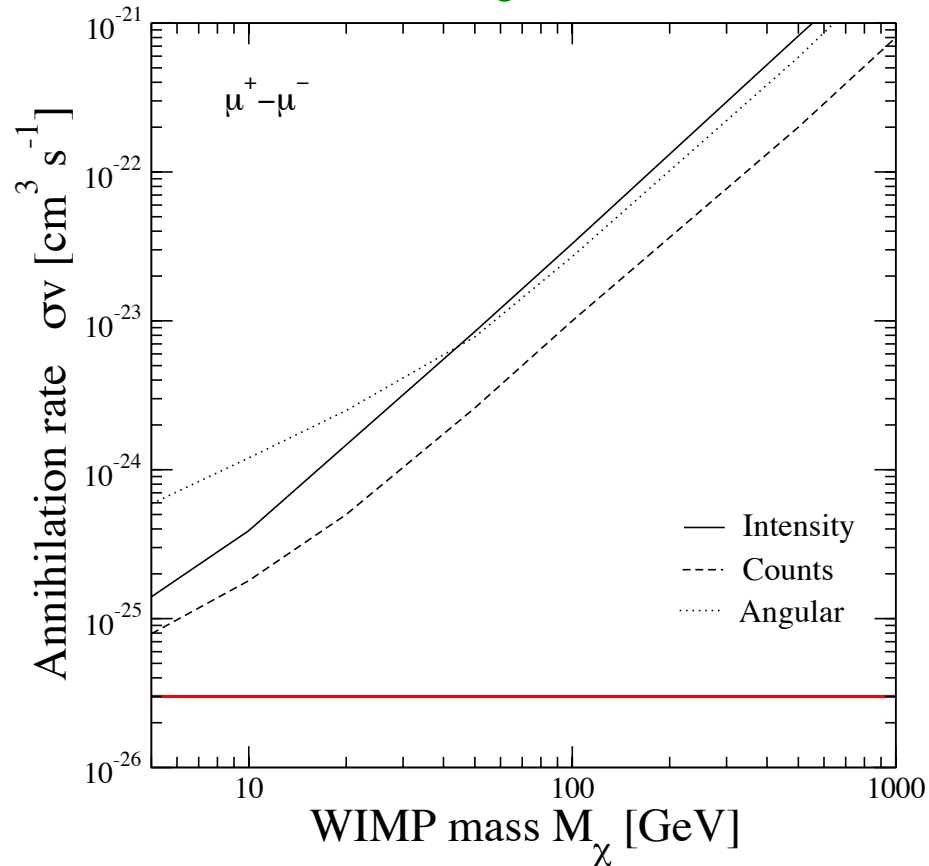


Bright sources: 1-halo term dominates, follows Poisson noise; astro sources dominate

Faint sources: 2-halo term dominates; DM dominates at low multipoles
(because DM contribution peaks at low z)

Constraints on DM properties

Annihilating dark matter



Intensity bound: subdominant (but see ARCADE discussion)
becomes more effective if low-brightness objects are included
(smaller M_{cut} / resolved substructures)

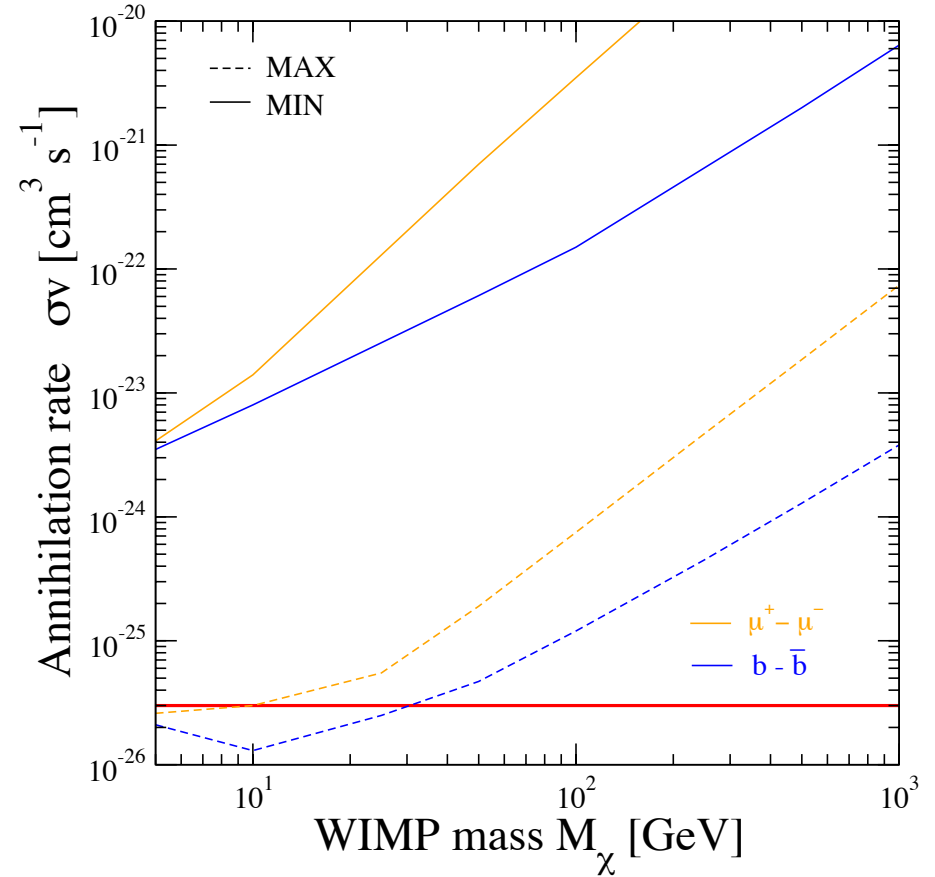
Future survey: are expected to improve considerably the bounds from number counts and anisotropies

Constraints on DM properties

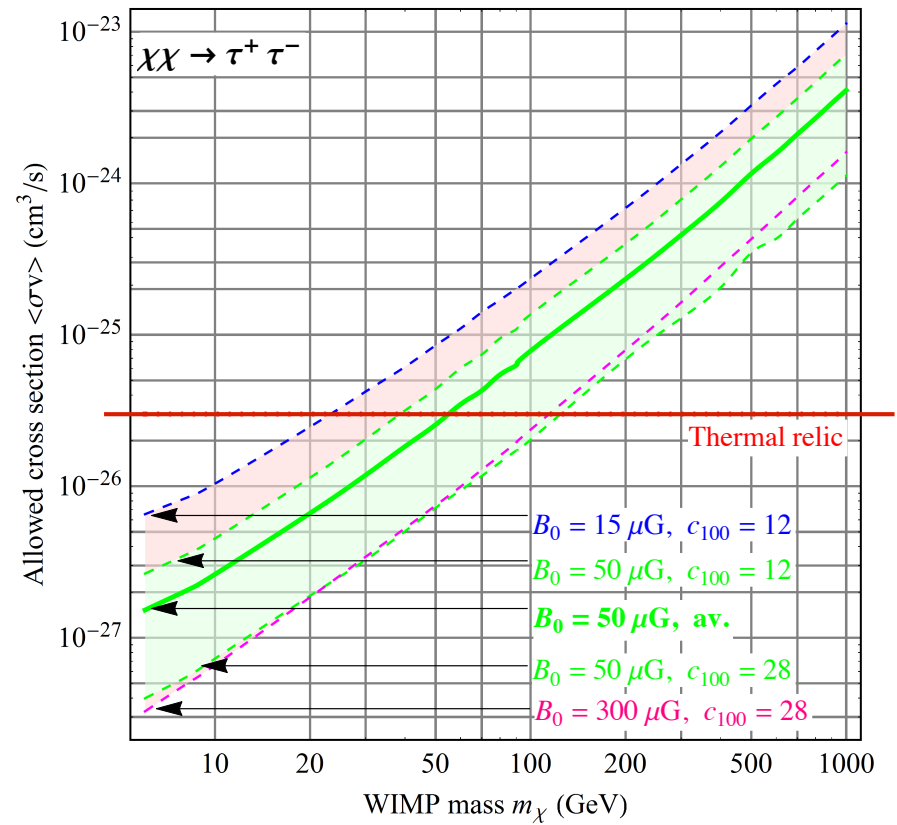
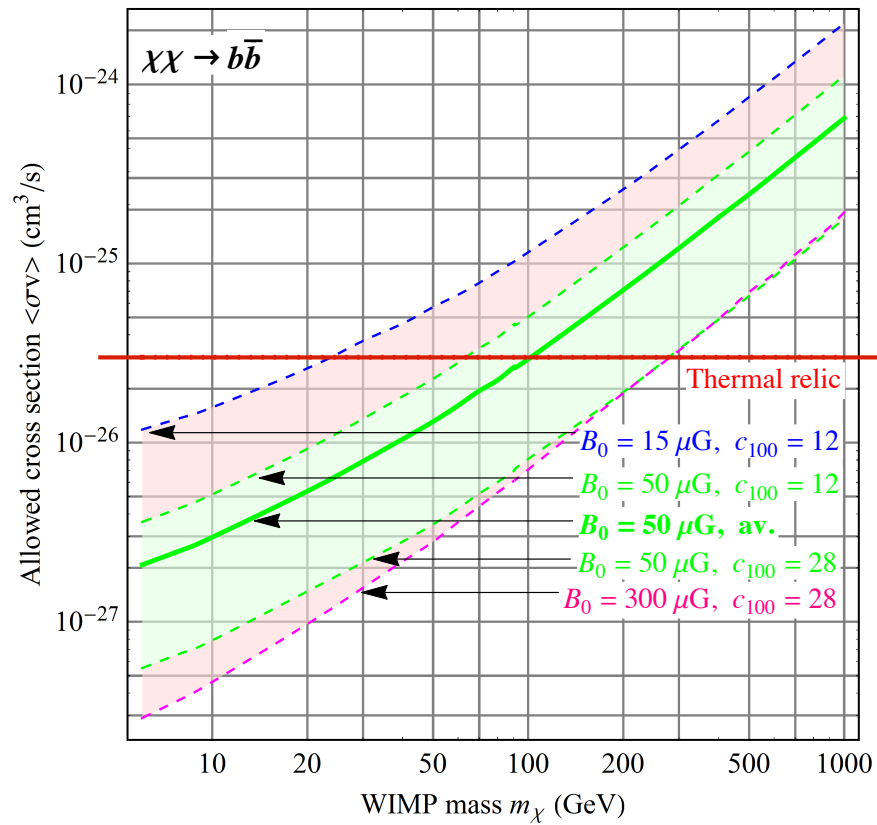
Annihilating dark matter

MIN: $M_{\text{cut}} \approx 10^6 M_{\text{sun}}$
 $B = B_0 (M/M_{\text{cut}})^{0.1} \exp(-r/(R_{\text{vir}}/50))$
 $B_0 \approx 10 \text{ microG}$
 electron escape
 no substructures

MAX: $M_{\text{cut}} \approx 10^{-6} M_{\text{sun}}$
 $B \approx B_0 \approx 10 \text{ microG}$
 electron radiate at injection point
 substructures not relevant with these params



Specific target: Andromeda



ARCADE excess

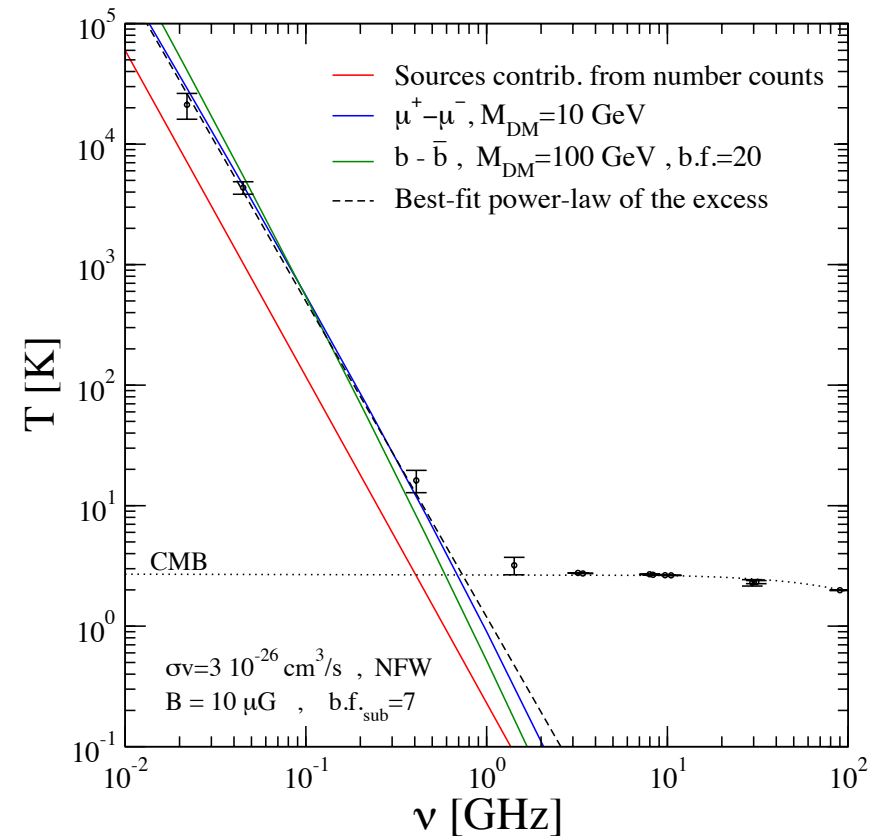
- After subtraction of an isotropic component, ARCADE reports a remaining flux (interpreted as extragalactic) **5–6 times larger** than the total contribution from detected extragalactic radio sources

ARCADE:

Singal et al., *Astrophys. J.* 730 (2011) 138

A. Kogut et al., *Astrophys. J.* 734 (2011) 4

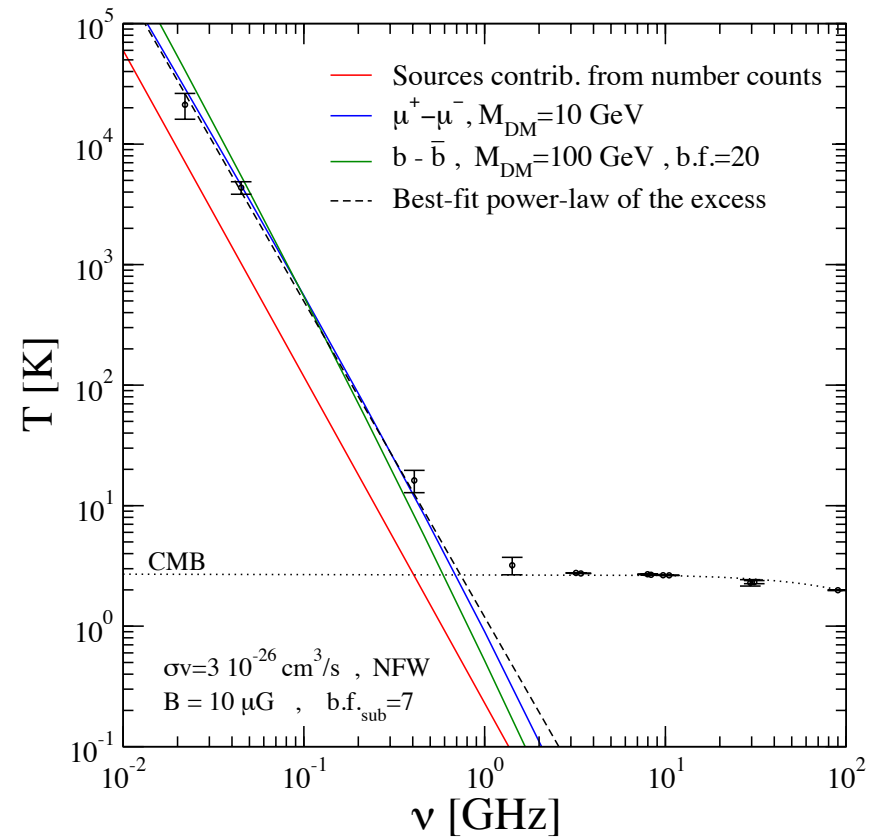
- Extrapolating the source number counts to lower (unreached) brightness, the excess remains
- Systematics effects and galactic sources seems excluded
- Such a level of radio extragalactic emission does not appear to have an immediate explanation in terms of standard astrophysical scenarios,, especially when multiwavelength constraints are applied
- A new population of numerous and faint radio sources (able to dominate source counts around μ Jy flux) has to be introduced



ARCADE excess

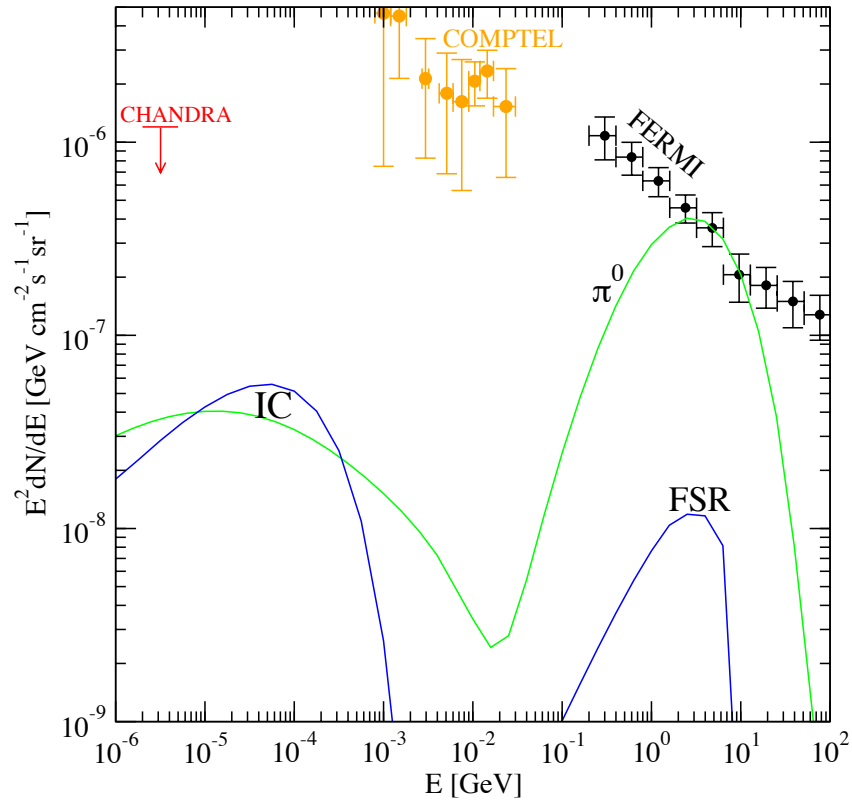
DM can easily explain the excess without special fine tunings

(Slight) preference for light (around 10 GeV) and leptophilic DM

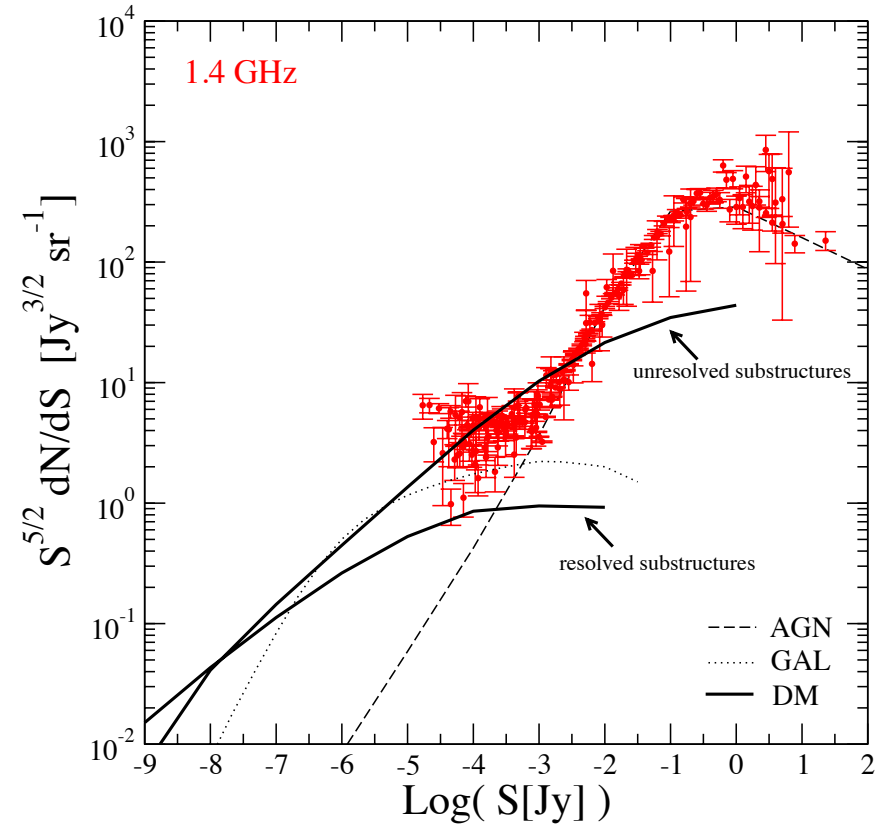


ARCADE excess

corresponding multiwavelength signals



differential number counts

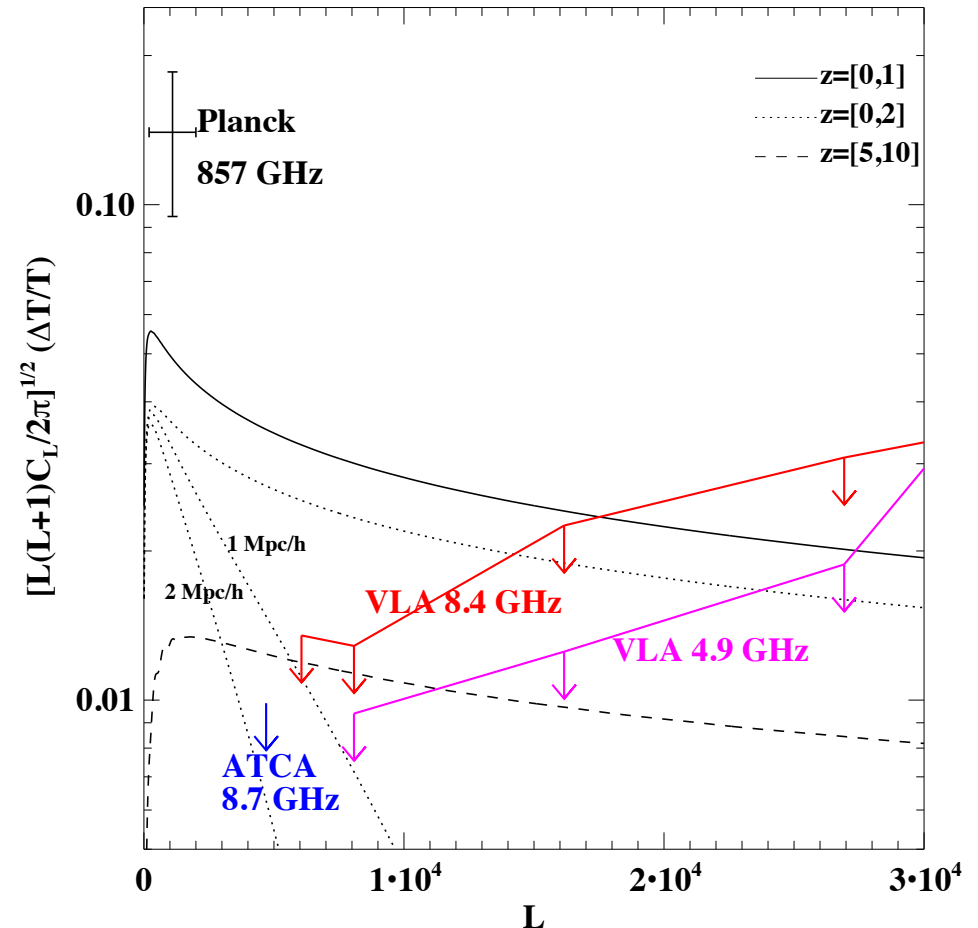


Fornengo, Líneros, Regís, Taoso, PRL 107 (2011) 27 [arXiv:1108.0569]

See also: Hooper et al., arXiv:1203.3547

Potential problem with EG interpretation

- Expected clustering at very large multipole and CMB frequencies, derived by rescaling the CMB anisotropy limits according to the ARCADE excess
- Derived bounds seem to imply that either:
 - Cosmological sources are at high redshifts ($z > 5$), where the clustering amplitude is smaller
 - Individual sources are spatially extended (few Mpc), to avoid clustering on arcmin scale



Holder, arXiv:1207.0856

New determination of the extragalactic T

- New analysis with a fit that uses a galactic emission model with a spheroid + sphere
- Extragalactic emission is found strongly reduced
- However: the scale of the spherical emission appears to be very large (about 20 kpc, compared to typical determinations of few kpc)

Table 1: Parameters that describe the decomposition of the all-sky maps.

	150 MHz	408 MHz	1420 MHz
Slope a_1 for a slab model	69 K	5.0 K	0.17 K
Intercept a_0	143 K	13 K	0.62 K
Semi-major axis ^a of the spheroid	1.60	1.56	2.1
Semi-minor axis ^a of the spheroid	0.29	0.24	0.37
Radius ^a of the sphere	2.39	2.14	1.8
Axial ratio of the spheroid	5.6	6.4	5.6
Brightness of spheroid in the plane ^b	69 K	7 K	0.79 K
Brightness of spheroid towards the poles ^b	12 K	1.1 K	0.14 K
Brightness of the sphere ^b	129 K	6.9 K	0.30 K
Background brightness from the optimization	21 K	4.5 K	0.14 K
Mean of the Markov chain sampling of the background brightness	28 K	2.5 K	0.12 K

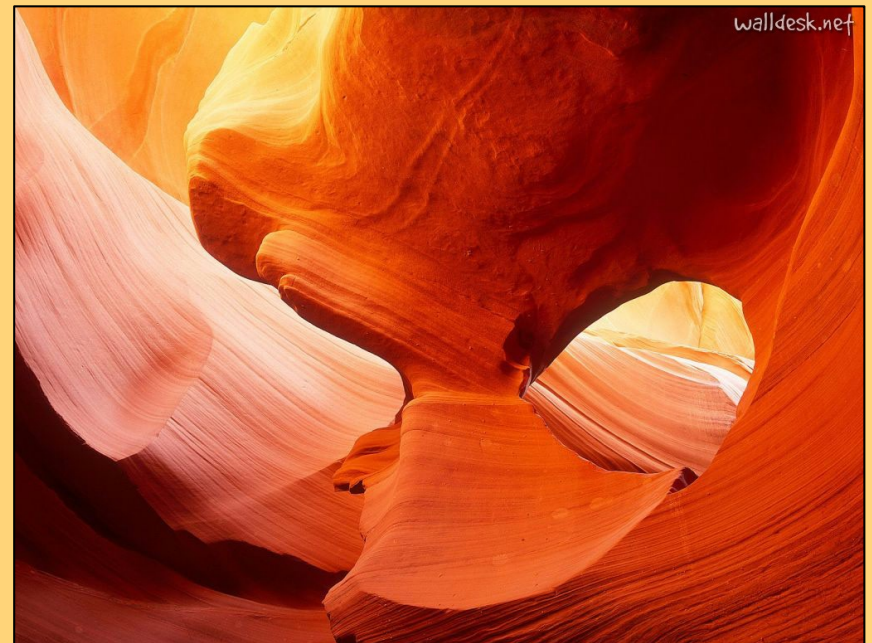
Subrahmanyan and Cowsik, arXiv:1305.7060

- Physical modeling of galactic emission required to assess the extragalactic T
- Preliminary results show that ARCADE excess is confirmed (*)

(*) Fornengo, Lineros, Regis, Taoso, in preparation

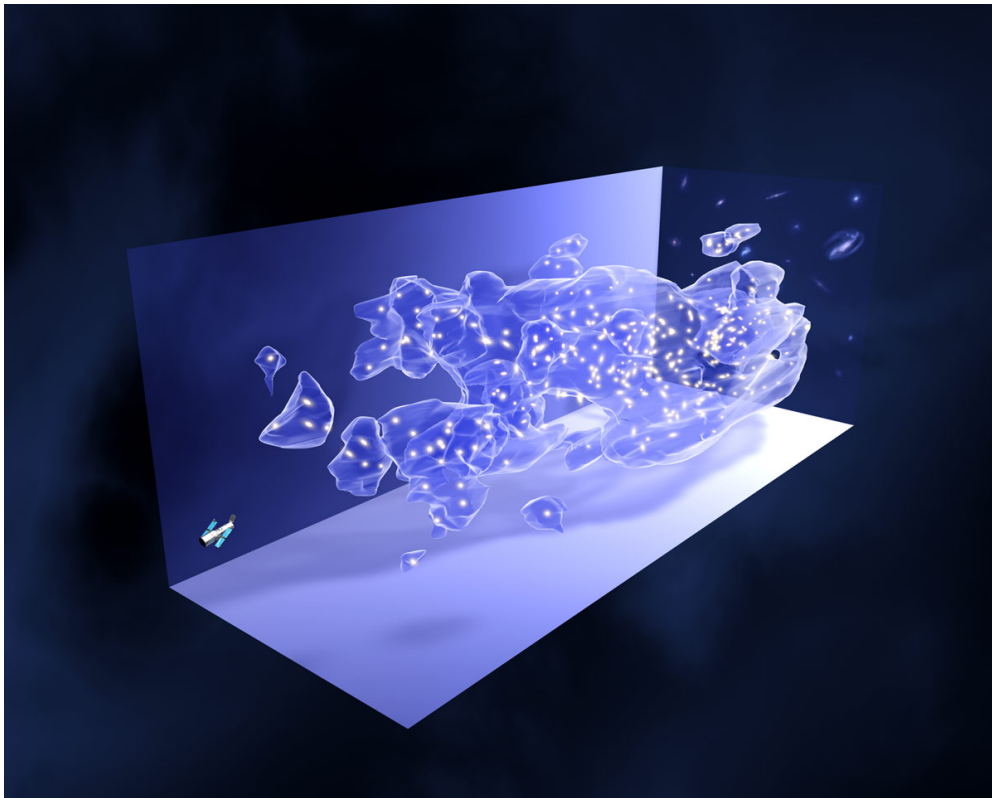
A NEW PROPOSAL:

**GAMMA RAYS/COSMIC SHEAR
CROSS CORRELATION**



Weak gravitational lensing

- **Weak lensing:** small distortions of images of distant galaxies, produced by the distribution of matter located between background galaxies and the observer









Powerful probe of dark matter distribution in the Universe

Weak gravitational lensing

Convergence: controls modifications in the size of the image

Shear: accounts for shape distortions

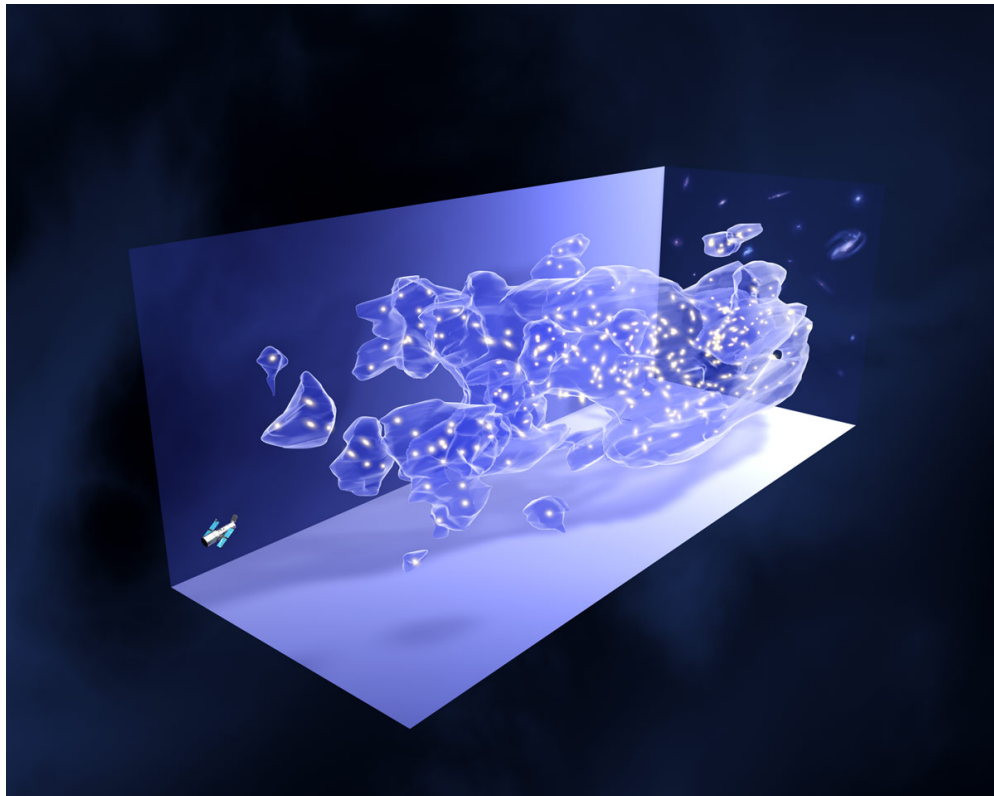
	< 0	> 0
κ		
$\text{Re}[\gamma]$		
$\text{Im}[\gamma]$		

In the flat-sky approximation, they generate identical angular power spectra

Cosmic structures and gamma-rays

The same Dark Matter structures that act as lenses can themselves emit light at various wavelengths, including the gamma-ray range

- ✓ From astrophysical sources hosted by DM halos (SFG, AGN)
- ✓ From DM itself (annihilation/decay)



Gamma-rays emitted by DM may exhibit strong correlation with lensing signal

Cross-correlation gamma/shear — Proposed in:

Camera, Fornasa, Fornengo, Regis
Ap. J. Lett. 771 (2013) L5 [arXiv:1212.5018]

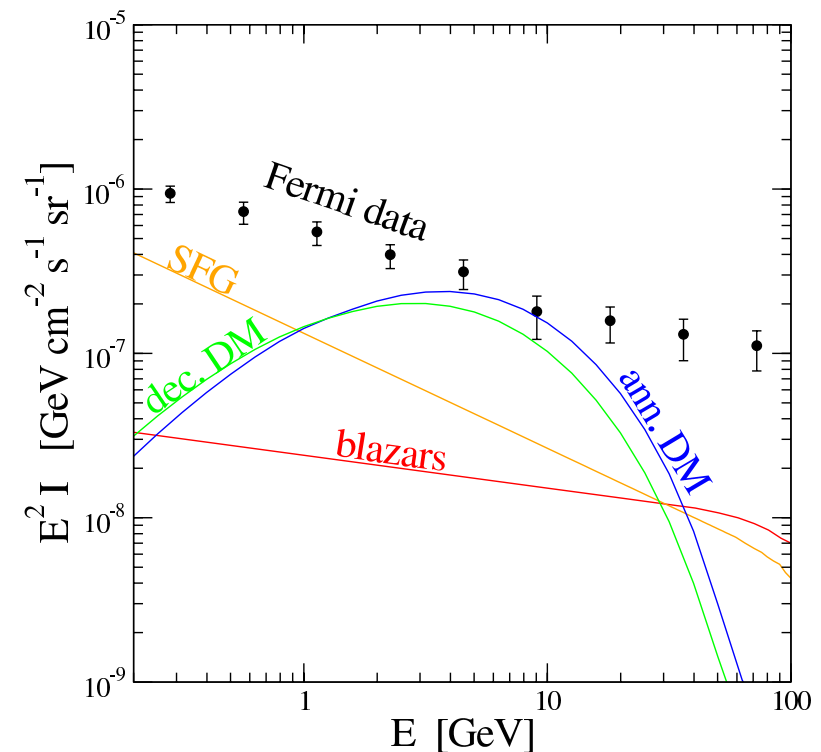
Extragalactic Gamma Rays Background

Most recent measurement comes from Fermi-LAT^(*)

EGB obtained by subtracting resolved sources and (modeled) galactic foreground

Unresolved sources (blazars, SFG, radio galaxies) contribute but actual amount is under study

DM may contribute to EGB
(very likely subdominantly)



(*) Abdo et al. (Fermi), Phys. Rev. Lett. 104 (2010) 101101

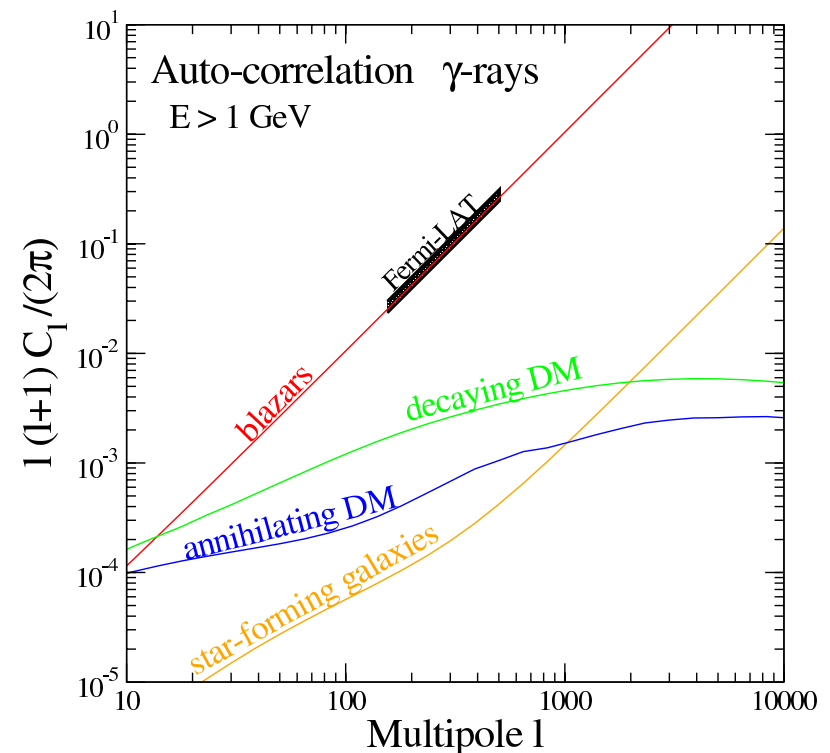
Gamma-rays auto-correlation

Auto-correlation in the gamma-rays emission has been reported (*)

For $l > 100$ galactic foreground can be neglected: EGB contribution

Features of the signal (energy and multipole independent) point toward interpretation in terms of blazars

DM likely plays here a (even more) subdominant role



(*) Ackerman et al. (Fermi), Phys. Rev. 85 (2012) 083007

Correlation functions

Source Intensity

$$I_g(\vec{n}) = \int d\chi g(\chi, \vec{n}) \tilde{W}(\chi)$$

Window function - depend on: source redshift-distribution for lensing
DM photon emissivity for gamma-rays
Density field of the source

Cross-correlation angular power spectrum

$$C_\ell^{(ij)} = \frac{1}{\langle I_i \rangle \langle I_j \rangle} \int \frac{d\chi}{\chi^2} W_i(\chi) W_j(\chi) P_{ij}(k = \ell/\chi, \chi)$$

3D Power spectrum

$$\langle \hat{f}_{g_i}(\chi, \mathbf{k}) \hat{f}_{g_j}^*(\chi', \mathbf{k}') \rangle = (2\pi)^3 \delta^3(\mathbf{k} - \mathbf{k}') P_{ij}(k, \chi, \chi')$$

$$f_g \equiv [g(\mathbf{x}|m, z)/\bar{g}(z) - 1]$$

\hat{f}_g : Fourier transform

1-halo term

$$P_{ij}^{1h}(k) = \int dm \frac{dn}{dm} \hat{f}_i^*(k|m) \hat{f}_j(k|m)$$

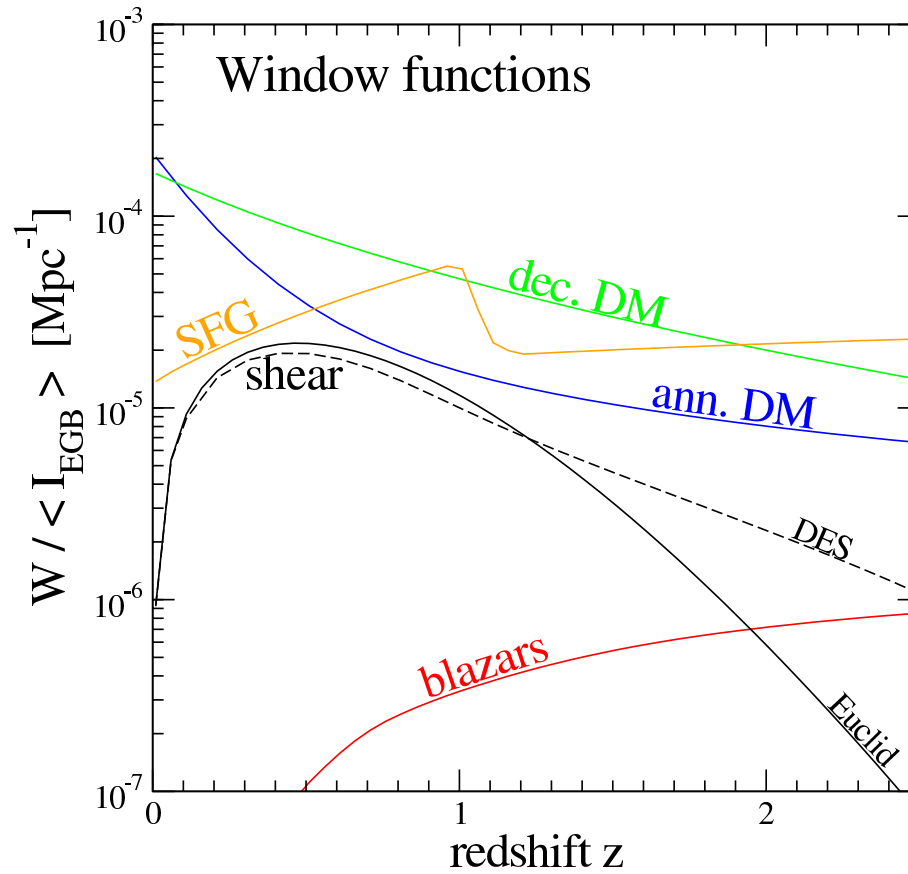
2-halo term

$$P_{ij}^{2h}(k) = \left[\int dm_1 \frac{dn}{dm_1} b_i(m_1) \hat{f}_i^*(k|m_1) \right] \left[\int dm_2 \frac{dn}{dm_2} b_j(m_2) \hat{f}_j(k|m_2) \right] P^{\text{lin}}(k)$$

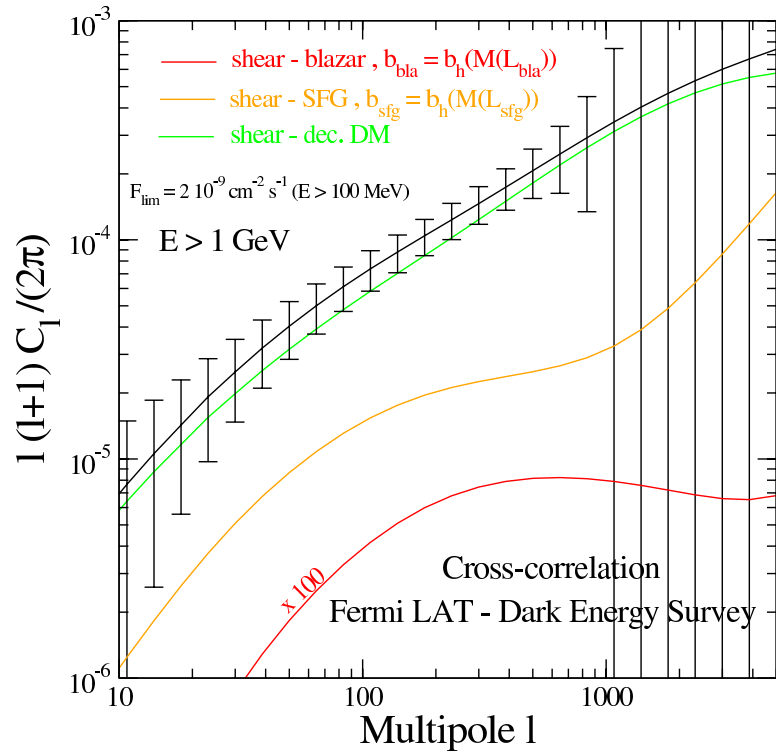
Linear bias

Linear matter PS

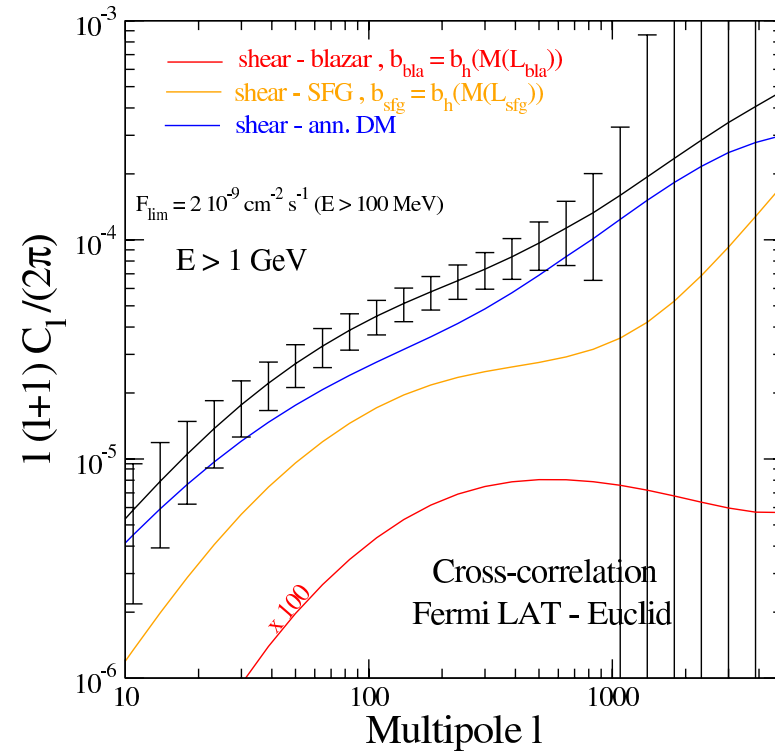
Window functions



Cross-correlation predictions

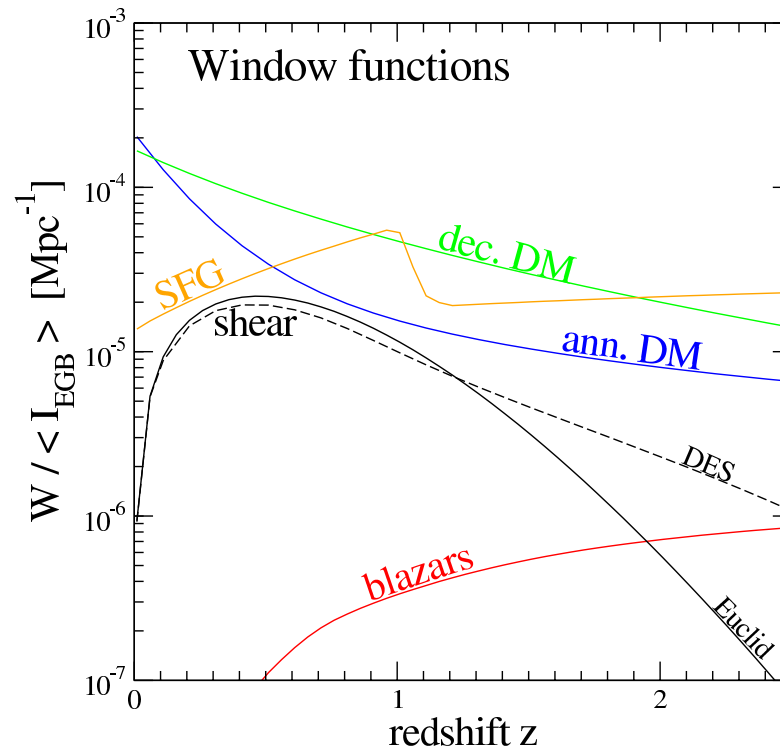
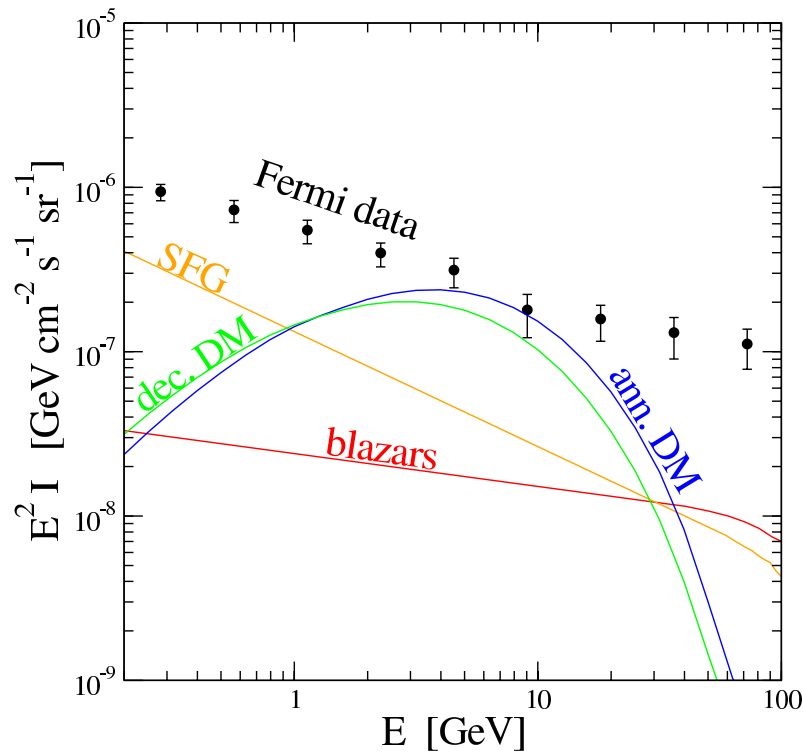


Fermi-LAT/5-yr with DES



Fermi-LAT/5-yr with Euclid

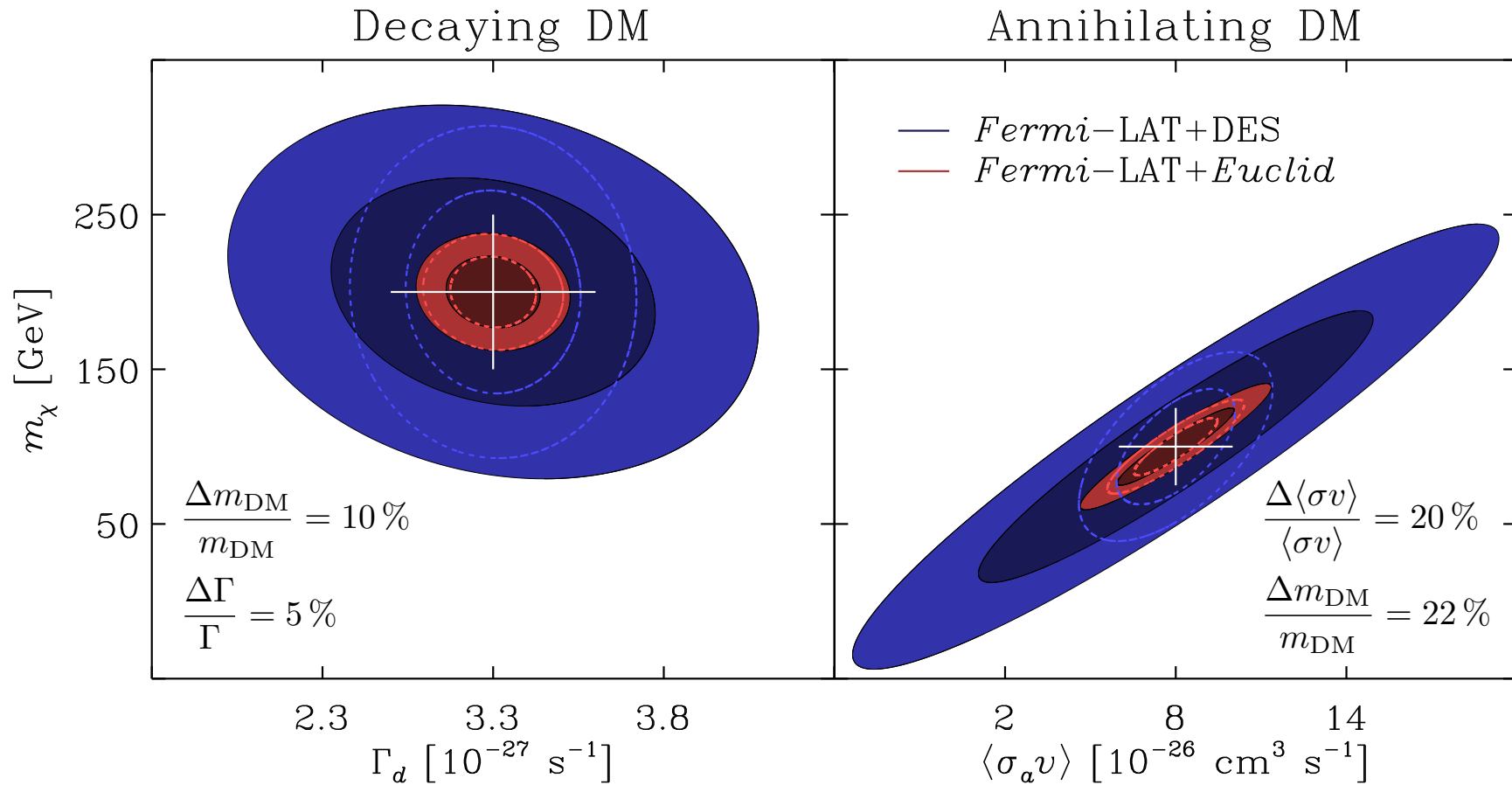
Energy slicing and Redshift tomography



Redshift information in shear: can be used to “separate” lensing sources

Energy spectrum of gamma-rays: can help in DM-mass reconstruction

Bayesian forecasts



Joint 68% 2-parameter error contours

Solid: gamma/shear cross-correlation
Dashed: includes also gamma auto-correlation

Camera, Fornasa, Fornengo, Regis, in preparation [preliminary plot]

Conclusions

- Multi-messenger and multi-wavelength signals offer a large network of opportunities for DM searches, which nicely complement direct detection investigation
- Galactic **antiprotons** (together with EG and dwarf-spheroidal gamma-rays) are currently setting the strongest bounds among the indirect detection searches
- Low-energy **antideuteron**s persist among the best opportunities for indirect-detection signal discovery (option of “background free” signal for AMS and GAPS for large portion of DM parameter space)
- **Radio** signals, notably at low frequencies, represent a promising channel, especially in view of the large sensitivities expected in future surveys (e.g. Lofar, SKA)
- Cross-correlations offer a new opportunity: **gamma-rays/cosmic-shear cross-correlations** have been shown to be a potential channel of discovery with the future weak-lensing survey (DES, Euclid)